SLAC-40
UC-28, Particle Accelerators
and High-Voltage Machines
UC-34, Physics
TID-4500 (40th Ed.)

EFFECT OF NUCLEAR RADIATION ON ORGANIC MATERIALS; SPECIFICALLY MAGNET INSULATIONS IN HIGH-ENERGY ACCELERATORS

March 1965

by

H. Brechna

Technical Report
Prepared Under
Contract AT(04-3)-515
for the USAEC
San Francisco Operations Office

Printed in USA. Price $3.00. Available from the Office of Technical Services, Department of Commerce, Washington 25, D.C.

ABSTRACT

The coil insulation on most magnets for use with accelerators consists of inorganic materials such as glass fiber and fillers impregnated with organic compounds such as epoxies, polyesters, and silicones. Many of the usual combinations are damaged if subjected to high radiation levels such as those anticipated at the Stanford Linear Accelerator, where the expected dose rate may be as high as 10^{11} rads per year.

This paper describes certain tests carried out at SLAC in which several commercially available insulations were found to deteriorate severely at total doses of as low as 10^{10} rads.

Changes in molecular structure induced by radiation effects and degradation of electrical and mechanical properties are discussed.

The development and testing of an insulation using pure Al_2O_3 fillers which have retained approximately 25% of its original mechanical strength at an absorbed radiation dose of 3.25×10^{12} rads will be described. This insulation requires minor changes in the usual winding and "potting" techniques prevalent in the industry. Interesting changes in the crystal structure of the filler are observed under irradiation.

TABLE OF CONTENTS

LIST OF SYMBOLS

A	atomic weight
A_x	beam cross sectional area
c	speed of light
D	irradiation dose
D	diffusion coefficient
E	energy
E_i	incident energy, energy at a depth i in material
E_o	particle energy
E_s	energy of scattered particles
I	beam current
I_o	scattered beam current
ℓ	shower depth
m_e	electron mass
N	Avogadro number 6.024×10^{23}
n	number of electrons
n_{max}	number of incident electrons
n_o	number of incident electrons at shower maximum
P	beam power
p	particle momentum
r	beam radius
r_e	electron radius
S	current density
t	time
v	electron velocity

LIST OF SYMBOLS - Continued

W	weight
X	radiation length
X_o	radiation length at shower maximum
Z	atomic number
α	fine structure constant $e^2/\hbar c$
β	v/c
γ	material density
ϵ_o	critical energy
σ	mechanical strength
θ	particle scattering angle
Ω	solid angle

LIST OF FIGURES

I. COIL INSULATION AND STRUCTURE

Coil insulation of high-energy water- or air-cooled magnets generally consists of a glass fiber woven fabric, with or without an additional layer of electrical insulation, such as mica, micapaper, or polyesterweb and organic binder or impregnant.

The glass fiber fabric (available in tape form) is wound around each individual conductor and around double pancakes and coil sections. Figure 1 shows basically the insulation structure of magnet coils. The coils are impregnated with suitable organic resins such as epoxies, polyesters, or silicones. Other organic resins, such as phenolics and polystyrenes, have superior properties, but due to manufacturing problems are not suitable for magnet coil insulations.

A. Fiberglass as Insulation Reinforcement

The fiberglass cloth used is lime alumina borosilicate, relatively free of soda (E-glass). The chemical compositions of E-glass cloth and a high strength S-glass are shown in Table I.[1]

TABLE I

CHEMICAL COMPOSITION OF GLASS FABRICS

Class type	Composition: %	SiO_2	B_2O_5	Al_2O_3	Fe_2O_3	MgO	CaO	Na_2O	K_2O	TiO_2
E-glass		54.5	8.0	14.1	0.8	4.5	17.0	0.6		0.5
S-glass		65		25		10				

The glass cloth is perfectly elastic and follows Hooke's Law to rupture. Fibers stretch approximately 3.5% maximum before breaking. These characteristics, as well as the mechanical, thermal and electrical properties of glass fibers listed in Table II, make the glass fabric very attractive as coil insulation.[2]

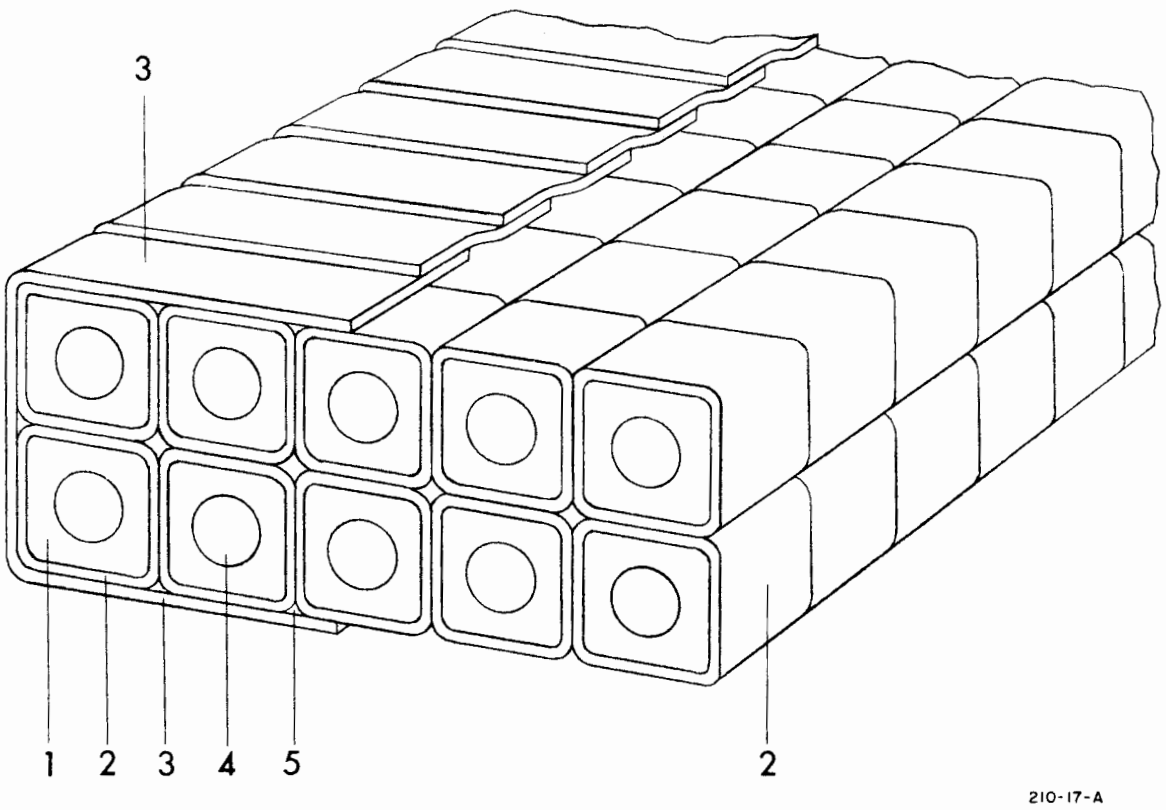

FIG. 1--Magnet coil configuration: (1) hollow conductor; (2) conductor insulation; (3) ground insulation; (4) cooling passage; (5) thermosetting filled space between insulations.

TABLE II

MECHANICAL, THERMAL AND ELECTRICAL PROPERTIES OF E-GLASSES AT 20°C

Tensile strength[a]	(kg/cm^2)	2.9×10^4
Tensile strength of glass fiber tapes (2.8×10^{-2}cm thick, 0.7 cm wide)	(kg/cm^2)	1.0×10^4
Compressive strength	(kg/cm^2)	$> 3 \times 10^4$
E-modulus	(kg/cm^2)	7.5×10^5
Specific gravity	(g/cm^3)	2.55
Specific heat	($Ws/gr°C$)	0.8
Heat conductivity	($W/cm°C$)	1.04×10^{-2}
Thermal expansion coefficient	$°C^{-1}$	4.8×10^{-6}
Heat distortion	(°C)	> 280°C
Volume resistivity	(ohm·cm)	10^{13} - 10^{15}
Dielectric constant		6.3
Fiber thickness	cm	$(3.8 - 9.7) \times 10^{-3}$
Cloth thickness	cm	available from: 2.54×10^{-3} to 5.08×10^{-2}
Radiation damage threshold	($ergs \cdot gr^{-1}$)	$> 10^{12}$

a) After 24 hours at 300°C the tensile strength is reduced to 80% of the original value, at 400°C to about 50%, at 500°C to 30%, and at 600°C to 20%.

In accordance with the type of insulation needed (conductor or ground insulation), glass fabrics are used in open, medium, or tight weave. Plain weave (yarn alternating under and over) and leno weave (two warp strands twisted around each fill strand) are preferred over unidirectional or other types of fibers.*

The large ratio of surface area to volume makes the glass cloth sensitive to attacks from chemicals and the fiber surface has great affinity for water. The glass manufacturing process makes use of starch-oil finishes on the glass surface, which, if used in combination with organic resins, do not result in maximum bonding strength between resin and fiber

*Certain manufacturers (Allis Chalmers) prefer unidirectional glass fiber tapes (B-staged) for coil insulation. These tapes (produced by Minnesota Mining and Manufacturing Co.) have been used in the last few years in combination with coil insulation.

In order to achieve maximum bonding, the glass is "heat cleaned" by a continuous oven process (570°C), or "batch heat cleaned" in rolls. In this case a maximum operating time temperature of 24 to 48 hours at 360°C is required to prevent development of rapid exotherm reaction in burning off the starch oil size. The tensile strength of fabrics is generally reduced 40-50% by heat cleaning.

In order to achieve maximum bonding to the resin, as well as to restore part of the loss in tensile strength due to heat cleaning, the glass fabric is chemically treated, which is known as a "surface finish." The surface finish is applied by a dip process and dried at temperatures which remove the water or solvents. The best surface finishes used commercially are Volan, Silane, and Garan. The chemical treatment restores the tensile strength up to approximately 75-80% of the original value. Chrome and silan chemicals associate themselves with the hydroxyl radicals of the glass, becoming firmly attached after the residual water is removed by drying. During subsequent laminating with an organic resin, organic groups on the surface will cross link to the active agents during the polymerization of the resins.

Volan A is a chrome chloride complex (methacrylato chromic chloride) which is adsorbed at about 0.13% by weight on the surface of the heat cleaned glass filament in fabric.

Silanes have the following general model structure:

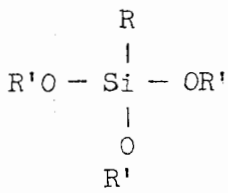

The solubility of silane in water depends upon the nature of the radicals R and R'. Alloxysilane complexes are applied to the glass surface by hydrolysis, vaporization at relatively low temperatures, and filtration techniques.

Alloxysilane with the simplified formula:

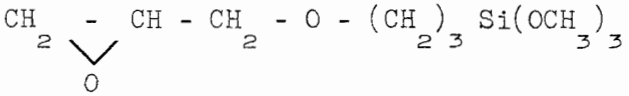

forms deposition centers on the glass surface from an aqueous solution due to the silane material. Optimum flexural and wet strength results occur at 0.1-0.8% silane loading. Wet strength retention of 70-90% is achieved after two hours boiling.

Garan finish is a vinylsilane complex.

B. Mica as Electrical Insulation

Micapaper has for several years been used for electrical insulation. Small mica splittings 0.1 ... 4 mm large and 4 microns thick are combined as a fleece or ground mica is bonded to glass fiber fabric with an organic binder. Micapaper and micafleece have excellent breakdown characteristics and their impregnation with organic resin is easy. Micafleece is produced: (a) by a thermal process from natural mica; (b) by a mechanical process (beam of water) from natural mica; (c) with synthetic mica (fluor phlogopite).

Micafleece manufactured by the mechanical process is used as electrical insulation. Mica types such as phlogopite and muscovite are the most suitable. Muscovite or potassium mica,

$$KAl_2\left[(OH,F)_2\,AlSi_3O_{10}\right]$$

is clear, transparent, or opaque. It shows signs of distortion at 500-600°C. Phlogopite or magnesium mica,

$$KMg_3\left[(OH,F)_2\,AlSi_3O_{10}\right]$$

is light yellow turning brown and is distorted at 1100-1200°C. Phlogopite is preferred because it is soft and elastic. Mica parts are applied to glass fiber cloth or tape with very little binder (3%). Mica glass tapes are also available with B-staged resins, with 25-30% binder by weight. If the tapes are dry, overlapping parts between mica pieces produce voids, which allow easy impregnation with organic impregnants. In the case of dry tapes one can expect 25% by volume voids (due to the overlapping of the mica plates), which will be filled with the organic resin.

In the wet type tapes the binder is heated and, due to the decrease of viscosity, flow uniformly over the tape, filling the voids and generating a uniform insulation around the conductor. Some of the interesting physical properties of mica insulation are given in Table III.

Mica has excellent radiation properties and its resistance against corona is well known.

TABLE III

PHYSICAL PROPERTIES OF MICAPAPERS

		Phlogopite	Muscovite
Width of micafleece	(m)	1	1
Specific gravity	(gr/cm^3)	1.7	1.7
Tensile strength (0.008-cm-thick and 5-cm-wide mica tape)	kg	1 - 2	0.5
Heat distortion	^oC	1100 - 1200	500 - 600
Melting temperature	^oC	1150 - 1350	1260 - 1290
Dielectric breakdown at 20^oC (0.01-cm-thick tape)	(kV/cm)	185	170
Radiation damage threshold	$ergs \cdot gr^{-1}$	$> 10^{12}$	$> 10^{12}$

C. Organic Resins

From a vast variety of organic resins we have chosen three thermosetting types, which have shown excellent physical properties and are used widely as magnet coil potting and impregnation resins.

1. Epoxy Resins

Epoxies are reactions of epichlorohydrin

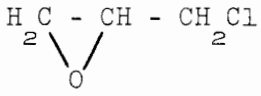

with a phenolic component such as bisphenol A:

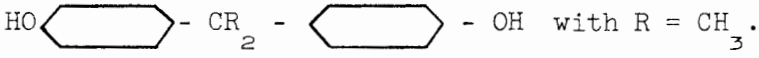

with $R = CH_3$.

They are linear polymers which cross-link to form thermosetting resins by virtue of reactions with curing agents such as diamines or anhydrides. The epoxide group is opened by means of a condensation type reaction, and subsequently a well-knitted polymer structure is formed without evolution of volatile by-products.[3]

Epoxies have low polymerization volume shrinkage (0.5 - 1%). Epoxies with no filler have low viscosity at impregnation temperature (50-100°C) and have an ultimate tensile strength of approximately 900 kg/cm^2; they have an excellent adhesive bond to glass fiber. The pot life of epoxies can vary between one hour to several days. Epoxies may cure at room temperature, but epoxies cured at high temperature show superior physical and radiation properties. The volume thermal expansion coefficient can be matched to the metallic conductor by adding to it suitable inorganic mineral fillers. Cured epoxies are generally hard, tough, and chemically inert. The internal toughness and durability of epoxies give them superior fatigue performance as compared to phenolic, unfilled polyester, and silicone laminates. The temperature range in which unfilled epoxies may be operated continuously is - 100°C to + 200°C. Filled epoxies have been used successfully up to - 269°C, without damage.

Table IV gives some of the important physical properties of epoxies. Physical properties of epoxies are changed if they are used in combination with glass fabrics and fillers. Table V illustrates the features of glass fiber reinforced organic resins. Cured epoxy resins normally have little affinity toward water and chemicals. However, tests with cured unfilled epoxy resins show absorption of water and an increase of weight. Water absorption is accelerated if the resin is heated. Figure 2 shows the mechanical properties of cured Araldite type B* placed in distilled water at elevated temperatures and exposed to water vapor. Figure 3 illustrates the acceleration of moisture absorption as a function of temperature. Glass fiber impregnated with epoxies shows more tendency toward water absorption. As can be seen from Fig. 4, the insulation resistance of vacuum impregnated glass fiber epoxy decreases rapidly when the insulation is immersed in tap water. However, surface-protecting

*Ciba trade name.

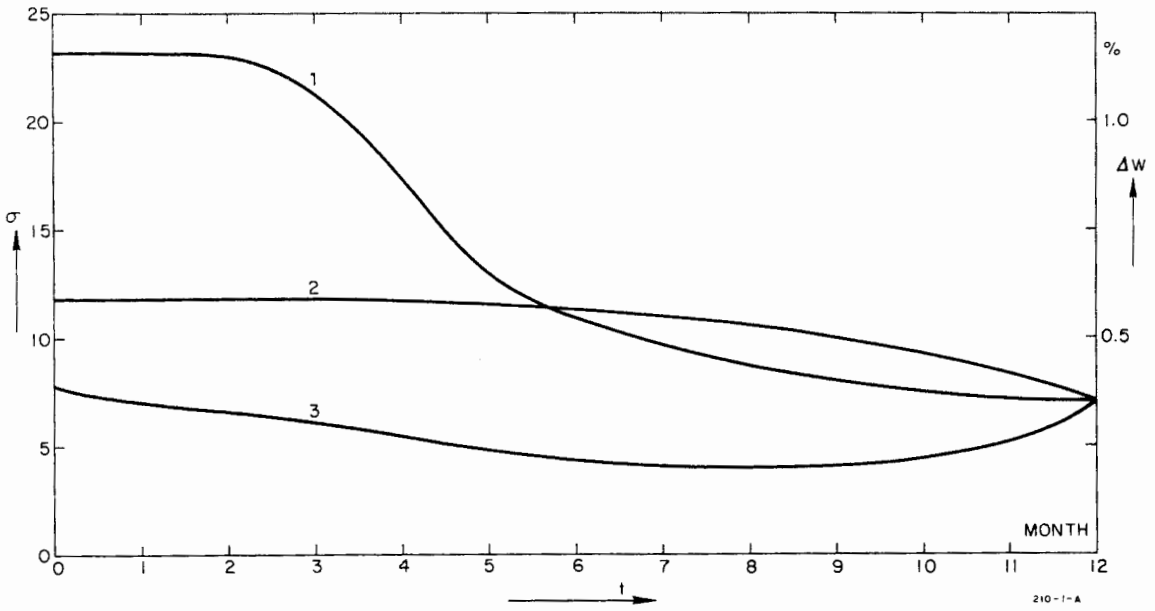

FIG. 2--Fatigue properties of araldite type B and curing agent 901 at temperature of 145-150°C. (1) Impact strength (cm gr/cm insulation thickness); (2) bond strength (kg/mm^2); (3) water absorption (%).
Observations: Samples were red-brown after one month, dark brown after three months, and black after six months and twelve months.

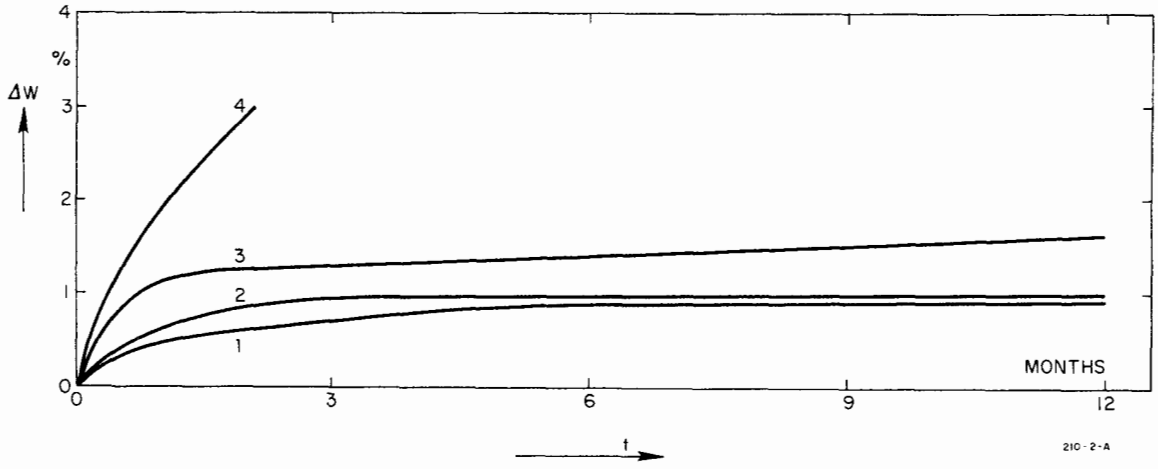

FIG. 3--Weight increase of epoxy type B and curing agent 901 (Ciba Chemical Corporation, Basle, Switzerland) due to water absorption. Samples were immersed in distilled water. (1) Water temperature 20°C; (2) water temperature 40°C; (3) water temperature 70°C; (4) water temperature 100°C.

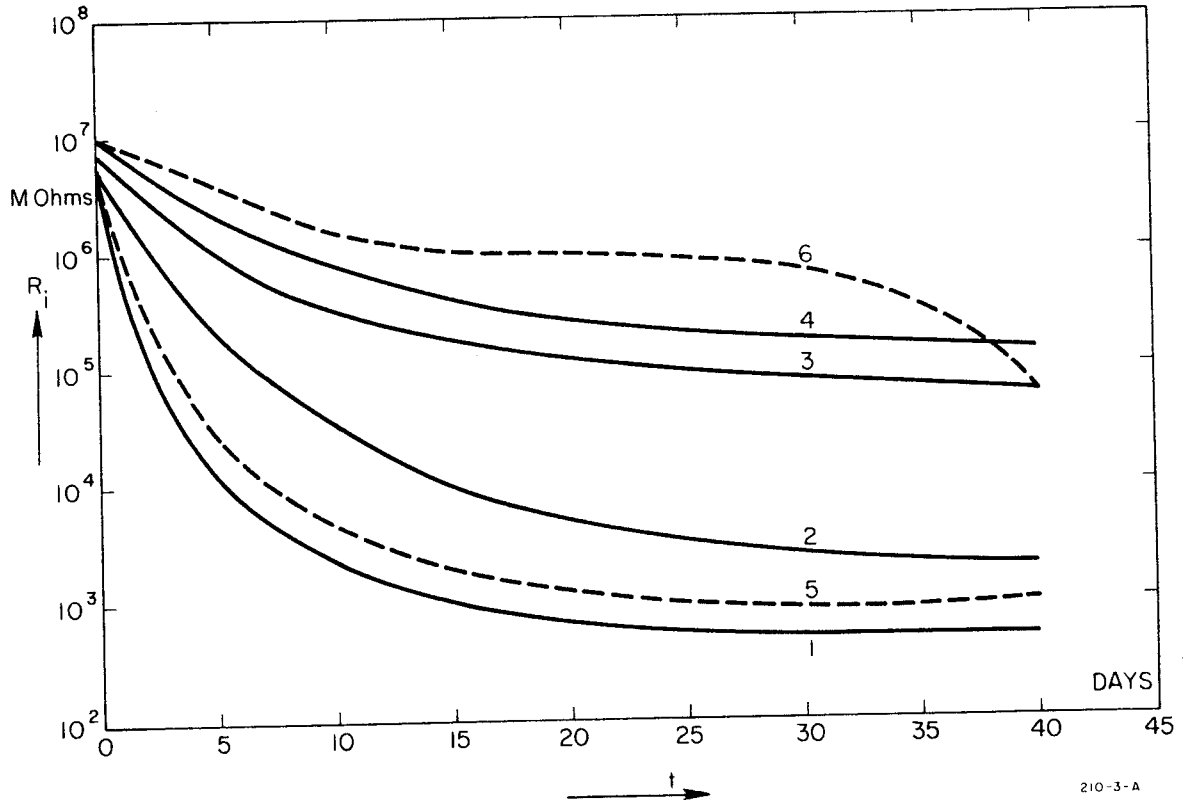

FIG. 4--Reduction of insulation resistance R_i as a function of water absorption. Test specimens were insulated with micafleece on Volan A treated glass fiber, medium weave, and vacuum impregnated with epoxy F and curing agent 905 (Ciba). Test pieces were immersed in tap water and were pulled out only during testing. (1) Mica-glass insulation and epoxy F 905 (glass fiber thickness 0.08 mm; micafleece thickness 0.05 mm; total insulation thickness 0.27 mm); (2) mica-glass insulation and epoxy F 905. A surface coating of polyester resin was applied to the samples; (3) mica-glass insulation and an additional top layer of polyester web tape. The whole assembly was impregnated under vacuum with F and 905; (4) Coil insulation according to the insulation technique used for curves 2 and 3; (5) coil insulation as for curve 4 (glass fiber thickness 0.1 mm; micafleece thickness 0.08 mm; total insulation thickness 0.4 mm); (6) insulation as for curve 4 (insulation thickness 0.65 mm).

organic coatings reduce water absorption, and after an initial fast drop, the insulation resistance remains constant.

2. Polyester Resins

Polyester resins are polybasic organic acids esterified with polyalcohols. The most useful resins are unsaturated and are used as solutions in unsaturated monomers. Polyesters cure by addition polymerization; they do not give off volatile components during curing and do not require pressure application as phenolic resins do. Such unsaturated polyesters have excellent physical properties in combination with coil insulation. The term "unsaturated" indicates that unbroken double bonds are carried over from the original ingredients (i.e., acids) into the finished resin to provide points of reactivity. The double bonds are opened by the catalyst. The final curing reaction (addition) is fulfilled with no by-product.

Polyester resins used for potting are liquid, or for coil insulation are B-staged. They may be operated up to 200°C. The volume shrinkage of polyesters compared to that of epoxies is quite high (5-8%), and the high thermal expansion coefficient [$(7\text{-}10) \times 10^{-4}$ cm/cm/°C] of polyester can be reduced by the addition of mineral fillers. Postcuring improves their temperature resistance.

A great disadvantage of polyester resins, which makes their use for coil insulation impractical, is their short pot life (a few minutes) at impregnation temperatures of 60°C. At room temperature the viscosity of polyesters is fairly high and makes uniform impregnation of woven glass fabrics difficult. The exothermic reaction of polyesters must be watched and controlled carefully.

As a comparison to epoxies, the physical properties of cast polyesters (unfilled and unreinforced) are given in Table IV.

The physical properties of reinforced polyesters are illustrated in Table V.

3. Silicone Resins

The term "silicone" is used to designate all organo-silicate materials. Generally these materials are organosilanes (SiH_4 and derivatives) or

TABLE IV

MECHANICAL, THERMAL, AND ELECTRICAL PROPERTIES OF CURED THERMOSETTING RESINS[a)]

Properties		Epoxies (no filler)	Polyesters (rigid type)	Silicones (low viscosity)
Tensile strength[b)]	(kg/cm^2)	280 - 900	500 - 800	200
Elongation	(%)	3 - 6	1 - 2	100 - 180
Young-E-modulus	(kg/cm^2)	2.5×10^4	$(4.3\text{-}5) \times 10^4$	1.4×10^4
Compression strength	(kg/cm^2)	$(1.07\text{-}1.5) \times 10^3$	$(1.4\text{-}1.7) \times 10^3$	800
Flexural strength	(kg/cm^2)	$(1 \quad \text{-}1.5) \times 10^3$	$(0.7\text{-}1.2) \times 10^3$	400
Impact strength, Izod	($cm \cdot kg/cm$)	11 - 54	11 - 27	10
Specific gravity	(gr/cm^3)	1.1 - 1.5	1.1 - 1.4	1 - 1.2
Specific heat	($Ws/gr \cdot {}^oC$)	1.05	1.2 - 2.0	1.5
Heat conductivity	($W/cm \cdot {}^oC$)	2×10^{-3}	1.7×10^{-3}	1.5×10^{-3}
Thermal expansion coefficient	($1/{}^oC$)	$(4.5\text{-}6) \times 10^{-5}$	$(7\text{-}10) \times 10^{-4}$	$(9\text{-}10) \times 10^{-4}$
Maximum heat of operation	(${}^oC$)	120 - 180	100 - 180	300
Heat distortion	(${}^oC$)	100 - 200	85 - 200	340
Volume resistivity	($ohm \cdot cm$)	10^{12} - 10^{14}	10^{14}	10^{13} - 10^{14}
Dielectric strength	($volt/cm$)	$(1.6\text{-}2) \times 10^5$	10^5	2.2×10^5
Viscosity of casting temperature	(cP)	150 - 600[c)]	1000 - 10,000	200 - 4000
Shrinkage during cure	(%)	0.5 - 3	5 - 8	0.3 - 1
Casting temperature	(${}^oC$)	20 - 140	25	20 - 25

a) The resins have a curing temperature range of 80 - 160°C (exception-silicones).
b) All data given, if not specified, are at 20°C.
c) Epoxy casting temperature is chosen conveniently to be 60°C.

TABLE V

MECHANICAL, THERMAL AND ELECTRICAL PROPERTIES OF MINERAL FILLED AND GLASS FIBER REINFORCED, CURED THERMOSETTING RESINS

Properties	Epoxies	Silicones (low viscosity)	Polyester (rigid type)
Tensile strength (kg/cm^2)	3900	1500	3200
Young-E-modulus (kg/cm^2)	$(2\text{-}4) \times 10^5$	2×10^5	2.1×10^5
Compression strength (kg/cm^2)	3500	1650	2500
Flexural strength (kg/cm^2)	5700	2850	4100
Impact strength, Izod ($cm \cdot kg/cm$)	80	27	100
Specific gravity (gr/cm^3)	1.6 - 2	1.5 - 1.8	1.9
Specific heat ($Ws/gr.^{\circ}C$)	0.8	~ 0.8	≈0.8
Thermal conductivity ($W/cm \cdot {}^{\circ}C$)	8×10^{-3}	1×10^{-2}	1.1×10^{-2}
Thermal expansion coefficient ($^{\circ}C^{-1}$)	$1.3\text{-}1.8 \times 10^{-5}$	$\sim 2 \times 10^{-5}$	1.6×10^{-5}
Maximum heat of operation ($^{\circ}C$)	200	300	200
Heat distortion ($^{\circ}C$)	220	370	220
Volume resistivity (ohm · cm)	10^{16}	4×10^{15}	10^{14}
Dielectric strength ($volt \cdot cm^{-1}$)	2×10^5	1.2×10^5	4×10^4
Viscosity at casting temperature (cP)	>1000	>2000	>2000
Shrinkage during cure (%)	0.2	0.1	0.5
Casting temperature ($^{\circ}C$)	60-140	25-30	25-30
Resin content by weight (%)	≈25-30	30-38	30-40
Insulation resistance (MΩ)	20,000	10,000	700

organo-siloxanes ($R_nSiO_{4-n/2}$). Final polymerization is accomplished by condensation of the silanol groups. Silicone resins range from flexible to rigid plastics. For coil insulation in combination with glass fiber fabrics, the rigid type is preferred. The big advantage of silicones is the high percentage retention of physical and electrical properties after prolonged exposure to temperatures of 200°C and over. Their somewhat lower mechanical strength (Table IV) is responsible for the fact that in most cases epoxies are preferred to silicones. However, properties such as resistance against corona, chemicals, moisture, and nuclear radiation make the rigid type, low viscosity silicones attractive. Filled silicones combined with glass fibers are used for magnet insulation. Table V gives a brief summary of reinforced silicone glass structures. Most organic resins lose their good mechanical properties at operating temperatures above 80°C-100°C. Silicones retain their properties up to 150°C-180°C. Figure 5 shows the tensile and compression strength of epoxies and silicones as a function of temperature.

D. Impregnation and Potting Techniques

Coil impregnation and potting techniques using organic resins are listed below.

1. Impregnation Under Vacuum in Closed Molds

The molds provide all-side uniform pressure to the coil surface and prevent the fluid resin from draining during the curing period. The molds and coils are preheated to the resin impregnation temperature. The recommended applied vacuum is less than 1 mm Hg. The best results with epoxies have been achieved at a vacuum of 400-600 microns. The resin systems are preheated to keep the viscosity down and are thoroughly degassed under vacuum prior to impregnation.

2. B-Staged Epoxies in Combination with Glass Fiber and Mica

The insulation tapes are loaded with 25-35% resin and kept refrigerated until they are used. After the coils have been taped, special mylar foils with a tendency to shrink at the curing temperature are wrapped around the insulation, and the coil is placed between heated metal plates and pressed into final dimensions until the resin is cured. Heating and

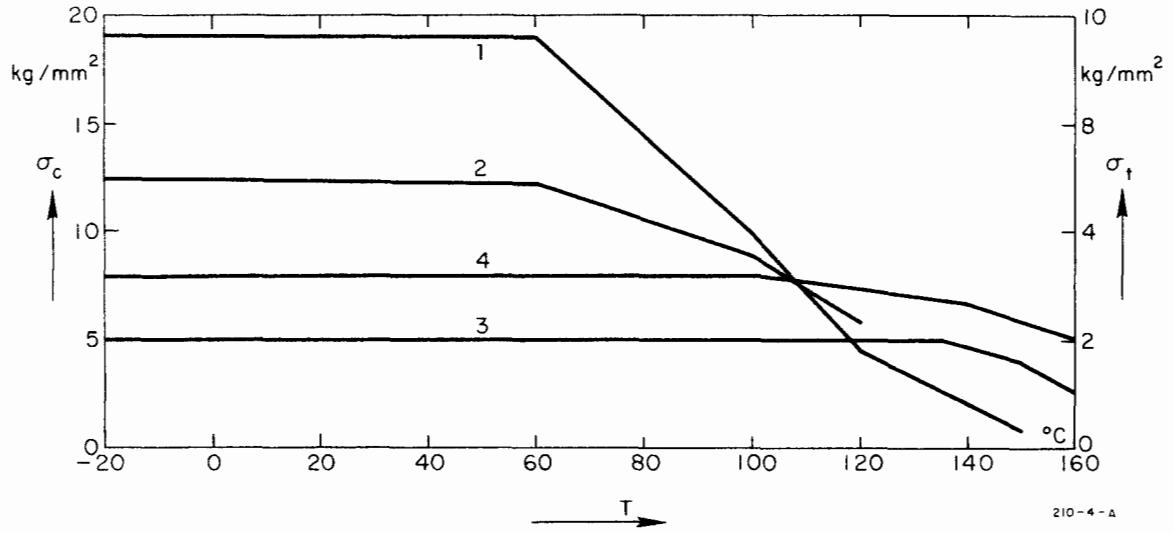

FIG. 5--Tensile and compression strength of araldite type B resin (Ciba), curing agent 901; and silicon resin R-7521, curing agent dicumyl peroxide and zircon filler at different temperatures. (1) Tensile strength σ_t(kg/mm^2) of epoxy; (2) compression strength σ_c(kg/mm^2) of epoxy; (3) tensile strength σ_t of silicone resin; (4) compression strength σ_c of silicone resin.

evacuation of the insulated coils prior to pressure application will improve the uniformity of the impregnation.

3. Mineral Filled Resins

To improve the compatibility of the resins with the conductor material, resins are loaded with inorganic fillers such as alumina, quartz, mica powder, talcum, or others. The increase of viscosity due to these fillers must be taken into account; therefore, the glass fiber cloth to be used in combination with these resins must be chosen adequately. Loaded resins can be used in either type (1) or type (2) insulations. The mechanical properties of filled resins are, as compared to pure resins, less advantageous, but filled resins still have adequate properties for coil insulations.

E. Stresses in Coil Insulation

The aim of designing suitable coil insulations is to provide a reliable product that will perform its intended function within the environment in which the magnet must operate. With the advancement of technology in high-energy accelerators, the demands on insulation have been increasing constantly. Coil insulations are subject to magnetic, electrical, and thermal stresses. The coil insulations have to be able to withstand the mechanical and thermal stresses over the expected lifetime of the magnet. Besides the requirement of reliability of the insulations, we ask also that the coils be able to withstand nuclear radiation, by placing the magnet in a radiation environment.

A short list of stresses may illustrate the most critical problems facing the coil insulation during operation.

1. Electromagnetic Forces

Electromagnetic forces due to self and induced fields cause stresses in the insulation.

2. Thermal Stresses

The operating temperature of conventional direct-cooled coils reaches about 100°C. The cooling water is heated while passing through the hollow conductors. The temperature gradient between adjacent conductors and pancakes causes shear, compression, and tensile stresses on the insulation.

3. Magnetic Field Fluctuation

Fluctuation of the magnetic field causes relative movements between adjacent turns and pancakes and leads to insulation rupture.

4. Insulation Breakdown

Surge voltage and overcurrent, which are constantly under mechanical and thermal stresses, may cause a rapid breakdown of insulation.

5. Moisture

Water vapor may cover the coil surfaces if the inlet water temperature is lower than the ambient room temperature. Moisture penetrates slowly into the insulation and causes breakdown.

6. Dust, Vapors and Chemicals

Physical properties of organic resins change slowly if exposed to chemicals such as SO_2, ozone, or acid vapors.

7. Corona Effects

Epoxies and polyesters are sensitive to corona and carbonize.

8. Radiation Effects

Coil insulations are affected by radiation, although small doses cause no significant effects. Organic materials (impregnants) are seriously affected, while the glass cloth, the inorganic fillers, and the ceramic parts (water pipes) are generally more resistant to radiation.

The irradiation effects on insulations are permanent and persist even after the radiation field is removed. The irradiation effect causes changes in the insulation structure, so that the magnetic, mechanical, and thermal stresses, even if they may be moderate, can cause damage. The irradiation effects which concerned us here are due to electron and neutron bombardments.

II. MAXIMUM EXPECTED IRRADIATION DOSE IN THE MAGNET INSULATION AS A FUNCTION OF THE BEAM ENERGY AND INTENSITY

A. Radiation Dose

When the charged particle traverses the combination of insulation and conductor material, it undergoes a large number of collisions, most of which produce small angular deflections. The discussion of the average behavior of showers represents a difficult mathematical problem and it was necessary to introduce simplifications wherever possible. The phenomena responsible for the development of showers are radiation and pair production processes in the electric field of the nuclei.

For the shower theory the variable collision loss is replaced by a constant collision loss ϵ_o, called the critical energy, which is the ionization loss per radiation length X_o.

We confine our attention to particle energies which are large compared with the critical energy. According to Rossi,[4] when

$$E_i \gg 137 \cdot m_e c^2 Z^{-\frac{1}{3}} \qquad (1)$$

the shower may be described by "Approximation B" which includes radiation, pair production and constant ionization loss.

For our case

$$m_e = 9.105 \times 10^{-28} \text{ gr}$$

$$Z = 29 \text{ (for copper)}$$

and therefore (for the maximum electron beam energy of 20 GeV at SLAC)

$$E_i = 20 \times 10^9 \text{ eV} \gg 137 \times 5.1079 \times 10^5 \times \frac{1}{(29)^{\frac{1}{3}}} = 2.286 \times 10^7 \text{ eV}.$$

The critical energy is

$$\epsilon_o = \left(\frac{dE}{dX}\right) X_o \qquad (2)$$

where (dE/dX) is the ionization loss of an electron of energy ϵ_o

and

$$\frac{1}{X_o} = 4\alpha \frac{N}{A} \cdot Z^2 r_e^2 \ln \left(183 Z^{-\frac{1}{3}}\right) , \qquad (3)$$

where X_o is the radiation length expressed in $gr.cm^{-2}$,

$$r_e = \frac{e^2}{m_e c^2} ,$$

the structure constant

$$\alpha = \frac{e^2}{\hbar c} = \frac{1}{137} ,$$

and

$$r_e = 2.8176 \times 10^{-13} \text{ cm.}$$

For copper conductors with

$$Z = 29$$

$$A = 63.54$$

we get from Eq. (3):

$$X_o \approx 13.0 \text{ gr/cm}^2.$$

For copper the critical energy is

$$\epsilon_o = 21.8 \times 10^6 \text{ eV}$$

The shower maximum in radiation length in Approximation B is calculated from the expression

$$\left(\frac{X}{X_o}\right)_{max} = 1.01 \left[\ln \frac{E_o}{\epsilon_o} - 1\right] . \qquad (4)$$

The average energy loss per particle by collison per unit length (gr/cm^2) is obtained from Eq. (2):

$$-\frac{dE}{dX} = \frac{\epsilon_o}{X_o} \tag{5}$$

where ϵ_o is the ionization loss per radiation length, or the critical energy.

Charged particles traversing the conductor lose energy by collision and by radiation. Electrons of high energy lose most of their energy by radiation. In the interaction of the electrons with the coil, only a small fraction of the energy is dissipated; the large part is spent in the production of high-energy photons. The secondary photons undergo Compton collision. This gives rise to electrons of energy comparable to that of photons. The new electrons radiate more photons, which materialize again into electron pairs. At each step the number of particles increases and their average energy decreases. This process continues until the energy of the primary electron is completely dissipated in excitation and ionization of atoms. The phenomenon outlined is called a multiplicative shower or a cascade shower. An analytic expression for the integral energy spectrum of a shower has been given by Tamm and Belenky[5]:

$$n = n_o \cdot \frac{0.31}{\left[\ln\left(\frac{E_o}{\epsilon_o}\right) - 0.37\right]^{\frac{1}{2}}} \cdot e^{\frac{X}{X_o}\left(1 - \frac{3}{2}\ln\frac{\frac{3X}{X_o}}{\frac{X}{X_o} + 2\ln\left(\frac{E_o}{\epsilon_o}\right)}\right)} \tag{6}$$

The gradual increase of X/X_o describes a progressive softening of the energy spectrum of the particles. At the shower peak the number of electrons can be computed from Eq. (6) to be:

$$n_{max} = n_o \frac{0.31}{\left[\ell n \left(\frac{E_o}{\epsilon_o}\right) - 0.37\right]^{\frac{1}{2}}} \cdot \frac{E_o}{\epsilon_o} \qquad (7)$$

where n_o is the incident number of electrons. Using Eq. (2) and Eq. (6), the ratio (n/n_o) as a function of (X/X_o) is computed for copper in Fig. 6 for different values of E_o.

Table VI gives the radiation length, the critical energy, and the ratio of $(n/n_o)_{max}$ and X_{max}/X_o for the electron incident energies of 20 GeV and 40 GeV.

Combining Eqs. (5) and (7), we obtain the relation (at shower maximum)

$$-\frac{n_{max}}{n_o}\frac{dE}{dX} = \frac{0.31}{\left[\ell n \left(\frac{E_o}{\epsilon_o}\right) - 0.37\right]^{\frac{1}{2}}} \cdot \frac{E_o}{X_o} \qquad (8)$$

Equation (8) multiplied with the beam current density in amps$\cdot$cm^{-2} and with E_o in eV, and X_o in g/cm^2 gives the power absorbed in watts/gram.

Calculating $-(n_{max}/n_o)(dE/dX)$ for 20 GeV/c electrons in a copper conductor (ϵ_o = 21.8 MeV) gives

$$-\frac{n_{max}}{n_o}\frac{dE}{dX} = 0.12 \cdot \frac{E_o}{X_o} = 1.85 \times 10^8$$

With the current density calculated for 30×10^{-6} amp average beam current and 0.30-cm incident beam radius (Fig. 7),

$$S_c = 1.06 \times 10^{-4} \text{ amp/cm}^2 ,$$

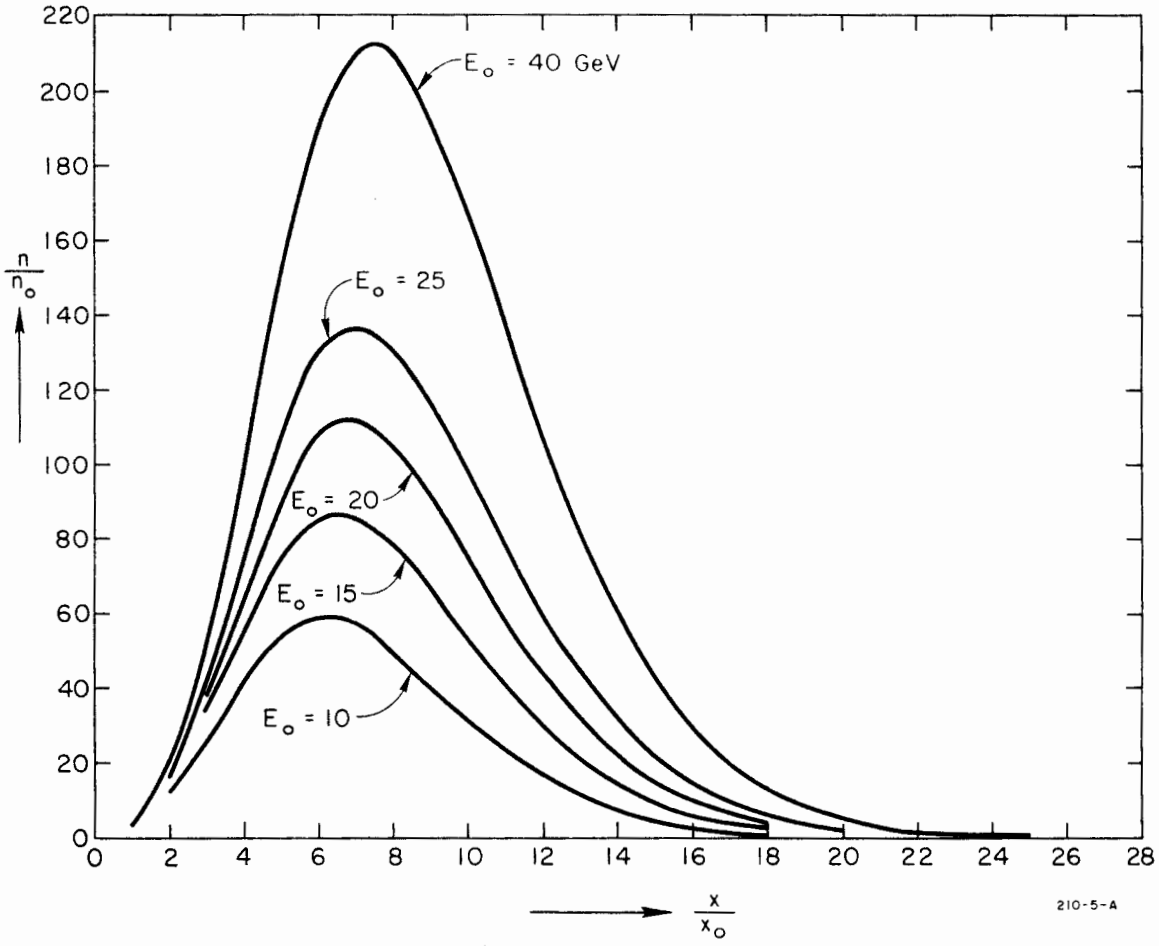

FIG. 6--Total number of electrons in a shower initiated by electrons of incident energy E_o in copper as a function of X/X_o according to the method of Tamm and Belenky (Approximation B).

TABLE VI

Material	X_o (gr-cm^{-2})	ϵ_o (MeV)	$\left(\frac{X_{max}}{X_o}\right)_{(20\ GeV/c)}$	$\left(\frac{X_{max}}{X_o}\right)_{(40\ GeV/c)}$	$\left(\frac{n_{max}}{n_o}\right)_{20\ GeV/c}$	$\left(\frac{n_{max}}{n_o}\right)_{40\ GeV/c}$
Copper	13.3	21.8	5.9	6.565	112	210
Mineral filled epoxy[a)]	25	50	5.04	5.74	52	99

a) Approximate values

we get the absorbed power

$$-\frac{n_{max}}{n_o} \cdot \frac{dE}{dX} \cdot S_c = \frac{\partial P}{\partial W} = 1.85 \times 10^8 \times 1.06 \times 10^{-4} = 1.96 \times 10^4 \text{ W/gr.}$$

The calculation of power density for the point beam gives excessive values. In fact, the high-energy beam has a physically realizable cross section and the calculation has to be modified for more realistic cases. The calculation of the power density for a diffuse source has been performed by Guiragossián[6] and considerations below have been adjusted according to our specific problem.

The point source Monte Carlo computation generates the energy density $E_{ij}(\text{MeV/cm}^2)$ due to shower electrons and photons, at a shower depth $(\ell_i - \ell_j)$ and over a radial interval $(r_i - r_j)$.

Because of the radial interval spacings and the rapid variation of the energy density, it was found that the direct fit of the Monte Carlo density distribution to an analytic form was not suitable.

Guiragossián used the numerical integration of $\partial E(r_i)/\partial \ell$ and used the SLAC computer program CURVE for generalized parameter fitting. The beam radial energy distribution is assumed to be Gaussian, and the result of $1/\gamma \cdot \partial P/\partial L$ in $\text{W/gr}\cdot\text{cm}^2$ is given in Fig. 7, curve 1, with γ as the density of copper and the incident beam energies of 20 GeV and 40 GeV, according to 10% beam loading for the Stage I and Stage II programs of SLAC.* The incident average beam power is accordingly 6×10^5 watts in Stage I and 2.4×10^6 watts for Stage II operation. The effective radial extension of showers as a function of the shower depth was estimated from 2π revolution of the Gaussian distribution. The effective area A_X for the cross section of the shower development as a function of L is given in Fig. 7, curve 5. The incident beam radius was taken to be $r_o = 0.3$ cm. The combination of curves 1 and 2 gives:

*According to SLAC specifications, the electron beam energy with 10% beam loading is 20 GeV in Stage I and 40 GeV in Stage II. The average beam current is 30×10^{-6} amps in Stage I and 60×10^{-6} amps in Stage II, with 2.1×10^{-6} sec pulse duration and the repetition rate of 360 pps.

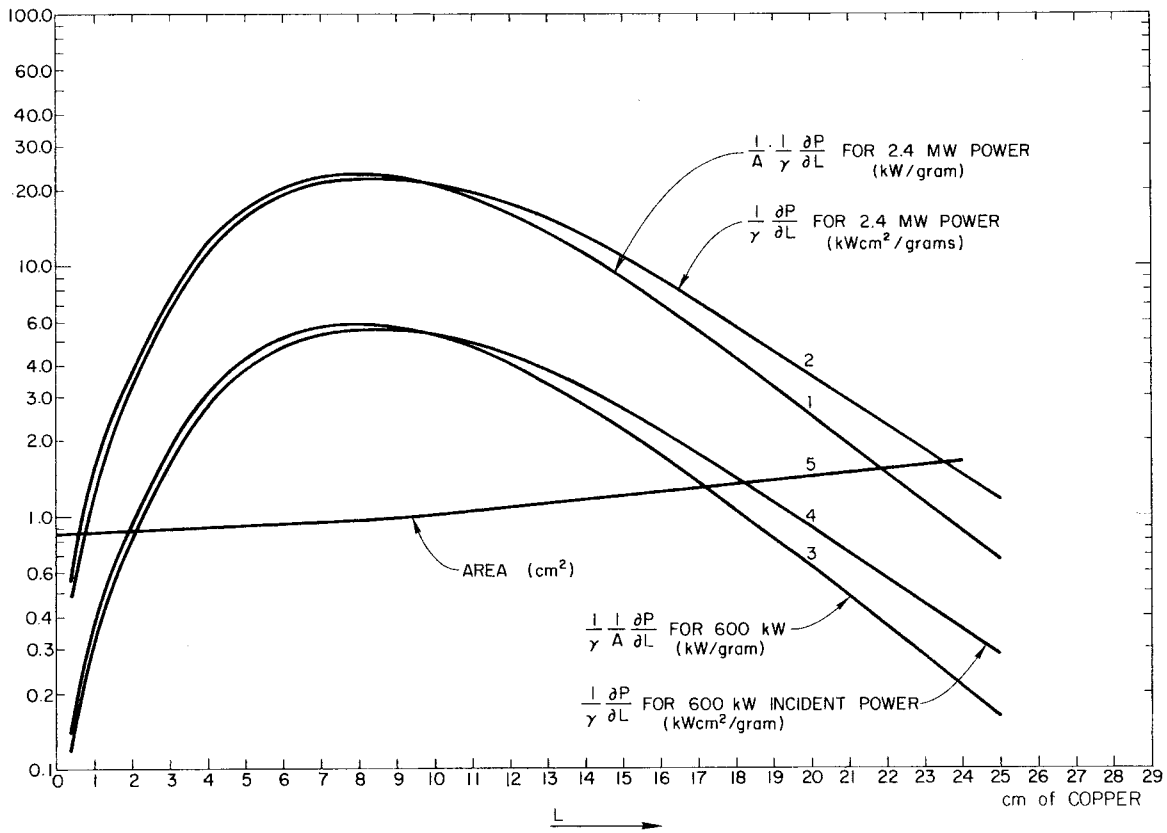

FIG. 7--Electron beam power distribution in a shower initiated by electrons of energy E_o in copper as a function of radiation length according to calculations by Guiragossián.

(1) $\frac{1}{\gamma}\frac{\partial P}{\partial L}$ (kW cm²/gr) for 2.4 MW incident beam power (corresponding to 40 GeV/c electrons)

(2) $\frac{1}{\gamma}\frac{1}{A}\frac{\partial P}{\partial L}$ (kW/gr) for 2.4 MW incident beam power; (3) $\frac{1}{\gamma}\frac{\partial P}{\partial L}$ (kW cm²/gr) for 600 kW incident beam power (corresponding to 20 GeV/c electrons); (4) $\frac{1}{\gamma}\frac{1}{A}\frac{\partial P}{\partial L}$ (kW/gr) for 600 kW incident beam power; (5) beam cross section A in (cm²).

$$\frac{1}{\gamma} \quad \frac{\partial P}{\partial L} \cdot \frac{1}{A_X} \quad (W/gr)$$

and is shown in curve 3, Fig. 7. At shower maximum the power densities at 20 GeV/c and 40 GeV/c are 5.84×10^3 W/gr and 23.3×10^3 W/gr.

If the beam can hit the coil for only 1 second before the interlocks shut off the accelerator, the total energy absorbed at shower peak would be 5.84×10^3 joules/gr (Stage I) and 23.3×10^3 joules/gr (Stage II). The heating of the coil due to beam energy is more effective than the degradation due to irradiation. Generally the magnets are not exposed to the full beam energy; they are protected by collimators, radiation shields, and slits. Only a fraction of the beam may hit the coils.

B. Elastic Scattering of Charged Particles

When the charged particle traverses through the conductors and coil insulation it undergoes a large number of collisions. Most of these produce small angular deflections. In order to calculate the angular deflection, Rossi[4] introduced a mean square angle of deflection, which is expressed as function X of the material traversed:

$$(\theta)^2_{\text{average}} = \left(\frac{E_s}{E_o}\right)^2 \cdot \frac{X}{X_o} \qquad (9)$$

with

$$E_s = \left(\frac{4\pi}{\alpha}\right)^{\frac{1}{2}} \cdot m_e c^2 \qquad (10)$$

where

$$m_e = 9.105 \times 10^{-28} \text{ gr}$$

$$\alpha = 1/137$$

we have

$$E_s \approx 21 \text{ MeV}$$

For our particular case, in Stage I,

$$(\theta)_{\text{average}} = \frac{21 \times 10^6}{20 \times 10^9} \cdot \left(\frac{X}{X_o}\right)^{\frac{1}{2}} = 1.05 \times 10^{-3} \left(\frac{X}{X_o}\right)^{\frac{1}{2}}$$

and in Stage II,

$$(\theta)_{\text{average}} = \frac{21 \times 10^6}{40 \times 10^9} \left(\frac{X}{X_o}\right)^{\frac{1}{2}} = 0.525 \times 10^{-3} \left(\frac{X}{X_o}\right)^{\frac{1}{2}}$$

With the definition of:

$$\frac{d(\theta^2)_{\text{average}}}{dX} = \theta_s^2 \tag{11}$$

we have

$$\theta_s^2 = \left(\frac{E_s}{E_o}\right)^2 \cdot \frac{1}{X_o} \tag{12}$$

and therefore:

$$(\theta^2)_{\text{average}} = \int_o^X (\theta_s)^2 \cdot dX$$

Let $I(\theta)d\Omega dX$ represent the probability that a particle of momentum p and velocity βc, traversing a thickness of dX, undergoes a collision which deflects the trajectory of the particle into a solid angle $d\Omega$ at an angle θ to its original motion. The expression $I(\theta)$ depends on the nature of the scattering material as well as on the charge and spin of the incident particle. For small deflection, the terms depending on spin become negligible and we can use the Rutherford scattering formula:

$$I(\theta)d\Omega = 4N \frac{Z^2}{A} \cdot r_e^2 \left(\frac{m_e c}{\beta p}\right)^2 \cdot \frac{d\Omega}{\theta^4} \tag{13}$$

Then θ_s can be written in terms of the scattered beam:

$$\theta_s^2 = \int \theta^2 I(\theta) d\Omega$$

$$= \int \theta^2 I(\theta)\, 2\pi\theta d\theta \ .$$

We now derive the scattered part of the beam (I_o) per solid angle:

$$\frac{1}{I_o}\frac{dI}{d\Omega} = \begin{cases} \dfrac{1}{\pi(\theta^2)_{\text{average}}} & \text{for } \theta^2 < (\theta^2)_{\text{average}} \\ \dfrac{(\theta)^2_{\text{average}}}{\pi\theta^4} & \text{for } \theta^2 > (\theta^2)_{\text{average}} \end{cases} \qquad (14)$$

C. Expected Irradiation Dose

In order to calculate the expected radiation level in a magnet coil located in the beam switchyard area of the Stanford Linear Accelerator, it was assumed that the coil is located 10 meters downstream from the collimator. The collimator allows 90% of the beam to pass unaffected. The remaining 10% will be partly scattered, partly absorbed. It was also assumed that the magnet and its coils are not protected by means of shielding or slits. The intensity of the scattered part of the beam decreases approximately (as was shown in Section B) with the fourth power of the deflection angle for $\theta > \theta_{\text{average}}$ and is approximately constant for small angles if $\theta < \theta_{\text{average}}$. If the radial distance of the coil from the beam axis is about 5 cm,

$$\theta = 5 \times 10^{-3}$$

For $X = X_o$, the mean square angle of deflection at a beam energy of E_o = 20 GeV was calculated:

$$(\theta^2)_{\text{average}} = 1.1 \times 10^{-6}$$

$$\theta_{average} = 1.05 \times 10^{-3} < \theta$$

From Eq. (14) we get:

$$\frac{1}{I_o} \cdot \frac{dI}{d\Omega} = \frac{1.1 \times 10^{-6}}{\pi \times 6.25 \times 10^{-10}} = 5.6 \times 10^{2} \text{ (steradians)}^{-1}$$

At 10m the current density of the scattered beam is

$$S_c = 5.6 \times 10^{-4} \; I_o \text{ (amp/cm}^2\text{)} \equiv I_o/A_{eff}$$

which corresponds to an effective area of $A_{eff} = 1780$ cm^2.

Using the charts for the power density per unit weight and recalculating the chart for an incident beam power of 60 kW (see Fig. 7), we get for $X = X_o$ and an area of 0.86 cm^2:

$$\frac{\partial P}{\partial W} = \frac{1}{\gamma} \; \frac{\partial P_{X_o}}{\partial X_o} \; \frac{1}{A_{X_o}} = 60 \text{ watts/gram}$$

The power density at the coil is reduced because the effective beam area is increased

$$\left(\frac{\partial P}{\partial W}\right)_{coil} = \left(\frac{\partial P}{\partial W}\right)_{Fig.\ 7} \cdot \frac{A_x}{A_{eff}} = 60 \; \frac{0.86}{1780} = 0.029 \; \frac{W}{g}$$

The power density per unit volume is

$$W_v = \gamma \; \frac{\partial P}{\partial W} = 0.26 \text{ W/cm}^3$$

The power density per cooling surface is calculated from

$$W_s = W_v \cdot \frac{\Delta V}{\Delta R} \approx 0.14 \text{ W/cm}^2$$

With a estimated bulk water velocity of $v_{H_2O} = 3\text{m}\cdot\text{sec}^{-1}$ we get a heat transfer coefficient between conductor and coolent of $h = 3.3$ W/cm^2 ^{o}C which gives a temperature rise in the boundary layer over the irradiation area of $\Delta\theta_{H_2O,bl} \approx 0.04$ ^{o}C. This shows that a small fraction of the absorbed beam energy is transformed into heat in the coil.

A very small fraction of the beam will be scattered. Assuming a magnet operation of 10 years with 8000 working hours per year, we may expect the total irradiation dose to be

$$D = \left(\frac{\partial P}{\partial W}\right)_{coil} \cdot t \cdot 10^7 \text{ (ergs/gr)} \qquad (15)$$

or, calculating the time t as

$$t = 10 \cdot 3.6 \cdot 10^3 \cdot 8000 = 2.88 \cdot 10^8 \text{ (seconds)}$$

we get

$$D = 0.029 \cdot 2.88 \cdot 10^8 \cdot 10^7$$
$$= 8.4 \times 10^{13} \text{ ergs/gr/10 years}$$

The problem is similar if energy slits are used. At these radiation levels, organic materials used in coil insulation degrade completely. A possible way to overcome this is to protect each magnet with an adequate radiation shielding, which requires space. Another possibility is to develop suitable insulations which have, at these high radiation levels, reasonably good electrical and mechanical properties.

However, as shown later, all commercially available organic materials degrade when exposed to radiation doses above approximately 10^{10} ergs/gr and lose their mechanical and electrical properties. Mineral fillers may improve the materials ability to withstand radiation up to approximately 10^{14} ergs/gr. Above these radiation levels we did not succeed in finding any satisfactory combinations of inorganic fillers with organic binders, and therefore recommend effective protection of coils by means of shielding.

III. IRRADIATION PROPERTIES OF ORGANIC MATERIALS

A. General Features

As pointed out in Section I, the magnet coil insulation consists of a supporting structure, i.e., glass fiber cloth, an organic binder, and an electric insulation in addition to the fiber glass, such as mica.

If the insulation is irradiated, the preliminary observations are:

First stage: Degradation and deterioration of the organic binder.

Second stage: Disintegration of mica from the glass cloth.

Third stage: Degradation of the glass cloth.

The different stages occur at different irradiation doses and each stage in this metamorphosis should be treated separately.

The organic binder consists primarily of carbon, hydrogen, oxygen, and perhaps nitrogen and halogen atoms bound together in various ways by covalent forces. Such covalent bonds can be ruptured by the addition of radiation energy. Organics differ from ceramics and metals in that the latter are primarily crystalline and generally do not contain covalent bonds; radiation does not effect them readily. At very high energy levels they show changes in their characteristics;[7] we do not concern ourselves in this paper with changes of electrical and thermal conductivities or annealing processes due to local build-up of heat. Due to the presence of covalent forces between atoms, plastics and organic binders are inferior to ceramics and inorganic materials. Radiation will induce chemical changes in polymers; where covalent bonds in molecular structure are broken, new bonds are formed and the structure is changed. Weaker bonds in the organic structure are ruptured first. The change in the molecule progresses until bonds of equal strength remain. Thus we may conclude that organic structures having only bonds of equal strength are most stable. Radiation effects in polymers are irreversible.

The changes in organic binders and impregnates may be classified under the following categories:

a. Permanent changes in appearance; color effects.
b. Chemical changes, such as double bond formation, crosslinking, oxidative degradation, polymerization and depolymerization, and gas evolution.
c. Physical changes, such as conductivity, crystallinity, heat distortion.
d. Mechanical changes, such as change in tensile and flexural strength, elastic modulus, hardness, elongation, and flexibility.

Several reactions may occur simulataneously under irradiation, but the initial effect is a "curing process" which improved tensile, flexural, shear, and impact strength by increasing cross-links. Radiation and heat are so efficient at this that the end result is always a binder so highly cross-linked as to be fragile and crash sensitive. At this point hardness and Young's modulus may be great, but the binder cannot withstand any mechanical stresses. The binder finally becomes brittle and

disintegrates into a black powdery substance. Irradiation makes the binder more susceptible to oxidation and moisture absorption.

Generally, not all properties of the organic binders are affected in the same degree. It is therefore possible to select materials which still have satisfactory electrical, mechanical and thermal properties at high radiation doses. The manufacturing problems of insulating play an important role in the choice of the material. For example, polystyrene is one of the most stable polymers, but its use in combination with coil impregnation is troublesome and the generated fumes are toxic.

A classification of polymers with respect to their stability against radiation is given in Table VII. From this table we may conclude that polymers containing benzene ring formations in side groups are the most stable ones. Therefore, "aromatic compounds" lend stability to polymers and "aliphatic structures" show poor radiation resistance.

Table VIII represents features of the most commonly used organic materials with coils. The data given are the results of a literature survey[7,8] and experiments carried on at an 80-MeV electron linear accelerator at Stanford (Mark IV). A 50% damaged polymer may still have adequate dielectric and mechanical properties in combination with magnet coils, but polymers show great affinity toward moisture absorption and fatigue readily. Coil insulations in this stage must be watched more carefully. However, in proper ambience they may still be quite useful.

It has also been found that:

1. Aromatic compounds are more stable (4-9 times) than aliphatic compounds, due primarily to the greater bond strength and the resonance energy of the aromatic structure. The evolved gases due to irradiation are again mainly hydrogen, with traces of methane and acetylene.
2. Substituted aromatics are more resistant than non-substituted aromatics.
3. Basic compounds are more stable than acid compounds because the bonds of COOH groups are relatively weak.
4. Saturated aliphatic structures are more stable than unsaturated aliphatic structures.

TABLE VII

POLYMER UNITS AND THEIR RESISTANCE TO RADIATION

Simplified Polymer Unit	Threshold Radiation Value (ergs/gr) unfilled resin	filled	Characteristics
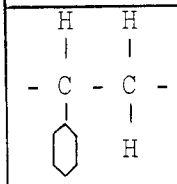	$10^{10} - 10^{11}$	-	Stable polystyrene with benzene ring in side chain (thermoplast)
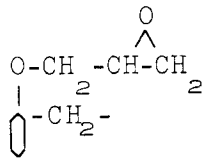	$(2\text{-}4.4) \times 10^{10}$	2×10^{11}	Epoxy chain with aromatic type curing agent
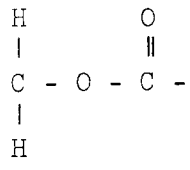	$10^{7} - 10^{8}$	10^{11}	Polyester chain
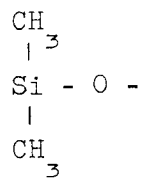	10^{10}	2×10^{11}	Basic silicone chain (dimethyl-silane)
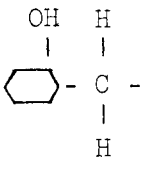	$10^{8} - 10^{9}$	4×10^{10}	Phenol formaldehyde polymer (increased cleavage due to radiation)
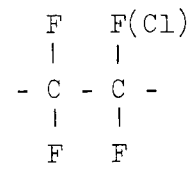	2×10^{6}	-	Teflon (poor radiation resistance)

TABLE VIII

RELATIVE RADIATION RESISTANCE OF THERMOSETTING RESINS AT ROOM TEMPERATURE

Resin	Radiation dosage ($ergs \cdot gr^{-1}$) required for:			
	threshold damage	25% damage	50% damage	90% damage
Epoxy				
Unfilled[a]	2×10^{10}	3.2×10^{11}	10^{12}	7×10^{12}
Laminated, glass fiber[b]	2.5×10^{11}	2.65×10^{12}	7.4×10^{12}	$\sim 2 \times 10^{13}$
Mineral filled[c]	10^{11}	5×10^{11}	3×10^{12}	$\sim 10^{13}$
Mineral filled and laminated, glass fiber	8×10^{11}	5×10^{12}	1.25×10^{13}	3.5×10^{14}
Polyester				
Unfilled[d]	5×10^{7}	1.2×10^{8}	5×10^{9}	-
Laminated, glass fiber[b]	8×10^{10}	5×10^{11}	10^{12}	-
Mineral filled	9×10^{9}	1×10^{11}	4×10^{11}	-
Silicone				
Unfilled[e]	10^{10}	4×10^{10}	2×10^{11}	-
Laminated, glass fiber[b]	1×10^{11}	10^{12}	6×10^{12}	-
Mineral filled	1×10^{11}	-	-	-

a) Epoxy: DER 332 LC and Epon curing agent Z or curing agent MPDA and MDA.

b) Medium weave, Volan A treated fiberglass.

c) Alumina, 900 mesh.

d) Unsaturated, low pressure, low viscosity polyester resin.

e) Silicone resin: R-7521, curing agent dicumyl peroxide and zircon filler.

5. Small molecules are more stable than large molecules.

6. Unbranched chains are more stable than branched chains.

In general, irradiation of aliphatic compounds results in a decrease of hydrogen content, evolution of gases, and lower temperature stability. The gases evolved are 60-95% hydrogen, with traces of methane and higher homologues. From tests performed at Oak Ridge,[9] it appears that there is little or no difference between the effects produced by various kinds of radiation on aliphatic hydrocarbons.

Generally, impregnants intended for high temperature use, such as phenolic epoxy types, have better resistance to radiation than the general purpose thermosettings. There is a distinct connection between radiation resistance and heat distortion temperatures. It is found that impregnants in combination with chemically treated glass fiber cloth have better radiation resistance than pure impregnants (Table VIII). Inorganic fillers improve the radiation stability of impregnants. However, the ratio of filler to impregnant and the type and grain size of the filler are important in achieving good results without sacrificing too much tensile and bond strength of the adhesive to the conductor.

Among the different resins, the following have been tested and their behavior is summarized briefly below.

1. Epoxy Resins

Radiation stability of epoxies is affected by the structure of the polymer, the curing agent used, the presence of a filler, and the reactive diluent. The fact is established that the greater the aromatic content, the greater the stability of the polymer. Thus, aromatic curing agents are superior to aliphatic curing agents. An epoxy polymer having a high heat distortion and a great number of aromatic groups is the most radiation stable impregnant. Epoxies with a high heat distortion temperature are more stable against radiation damage.

A distinct connection between radiation resistance and the "strength of char" also exists. Mixtures of different epoxies (see below) blended with aromatic amines result in charred compositions with two to three times the strength of one epoxy blended with aromatic curing agents. These mixtures also have higher radiation resistance.

Glass fiber reinforced epoxy resins combined with inorganic fillers are far superior to pure polymers. Table VIII gives relative values of radiation damage for a number of epoxies, filled and unfilled. Tests carried out at the Mark IV accelerator showed an improvement by a factor of 12 for the filled epoxies as compared to glass fiber reinforced epoxies. High temperature epoxy impregnated glass fibers with 50-75% mineral filler by weight of the impregnant have a threshold value of 2×10^{12} ergs/gr. At higher radiation doses the binder disintegrates to a black powder, but the filler-glass cloth structure retained at 3×10^{14} ergs/gr about 18% of the initial insulation tensile strength.

2. Polyester Resins

Unfilled polyester resins have poor radiation stability. They harden under irradiation and develop small cracks. Newly developed polyesters have better stability, but their properties begin to change at $(1\text{-}5) \times 10^{8}$ ergs/gr. Tensile, flexural, and impact strength decrease (see Table VIII). The addition of inorganic fillers improves the radiation properties by a factor of 100.

Combination of polyester resins with glass fiber cloth and mineral fillers does not improve considerably the radiation stability (compared to filled polyesters), but it improves the strength of the structure.

3. Silicone Resins

Silicone resins generally have a high phenyl content and therefore have a reasonably good radiation stability. Silicones are not seriously degraded at exposure doses up to $10^{9}...10^{10}$ ergs/gr. The use of proper inorganic fillers may improve their properties by a factor of 50. Glass fiber reinforced, mineral filled silicone resins have a threshold value of 10^{11} ergs/gr and rank among the best materials available (Table VIII).

The radiation stability of the above resins is affected if the insulations are additionally exposed to heat, water and water vapors, and chemicals. A large number of tests have been performed with resins exposed to radiation and ambient influences.[7,8,9]

However, in coil insulations, the effect of water vapors and temperatures up to 100°C and dielectric stresses have to be considered in combination with radiation effects. Tests performed with the Mark IV

accelerator showed that the presence of water vapors did not affect the mechanical properties, but it reduced the dielectric strength of the glass fiber, filled epoxy structure considerably.

In general, the dielectric properties of tested resins do not change considerably up to total radiation doses of 10^{12} ergs/gr. A reduction of 42% in insulation resistance could be measured in glass fiber, epoxy impregnated structures. Even at the very high dose of 10^{14} ergs/gr, where the organic binder has been completely degraded, the insulations show sufficient insulation resistance at room temperature and dry air. The insulation resistance decreases rapidly if the insulation has been exposed to moisture and water vapor.

B. Insulations with Organic Thermosettings

The results of tests carried out on organic resins and on glass fiber reinforced organic impregnants are given below. The setup of the samples and test equipment is shown in Fig. 8 and Fig. 9. In order to eliminate excessive local build-up of heat due to radiation energy absorbed by the sample, hollow water-cooled copper conductors were used. The conductors were cleaned thoroughly with a mixture of acetone and trichlorethylene and sanded.

The polymer to be tested was preheated and degassed, and the cleaned conductors were preheated to the temperature of the polymer.

The organic binder was applied to the conductors in the following ways:

1. Adjacent conductors were heated and bonded under 3.5 kg-cm^{-2} pressure to each other. The cured bonding film had a thickness of 0.005-0.008 cm (Fig. 8a).
2. Each conductor was wrapped individually with glass fiber cloth (half-overlapped Volan A treated, 0.017-cm-thick, medium weave). The conductors were impregnated under a vacuum of 0.04-0.05 mm Hg in a closed mold and cured under specified temperature, while pressure was applied to them constantly by the cover and side walls of the mold (Fig. 8b).

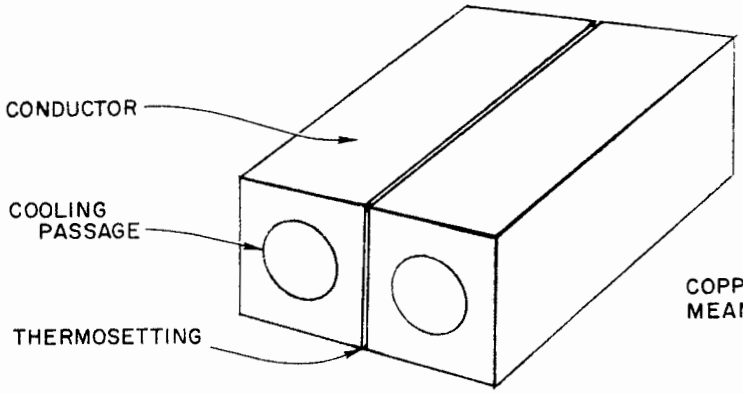

(a)

COPPER CONDUCTORS BONDED BY MEANS OF A THERMOSETTING.

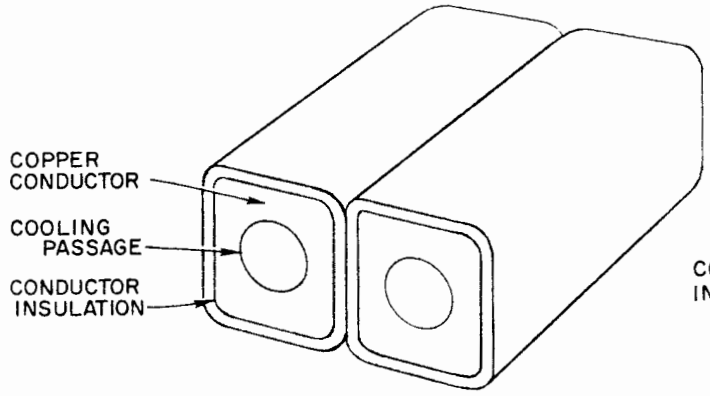

(b)

COPPER CONDUCTOR WITH CONDUCTOR INSULATION.

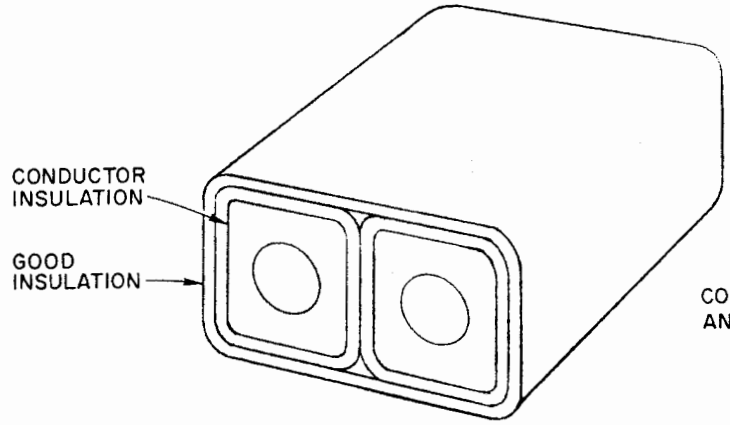

(c)

COPPER CONDUCTOR WITH CONDUCTOR AND GROUND INSULATION.

210-18-A

FIG. 8 - SAMPLE FOR IRRADIATION TESTS

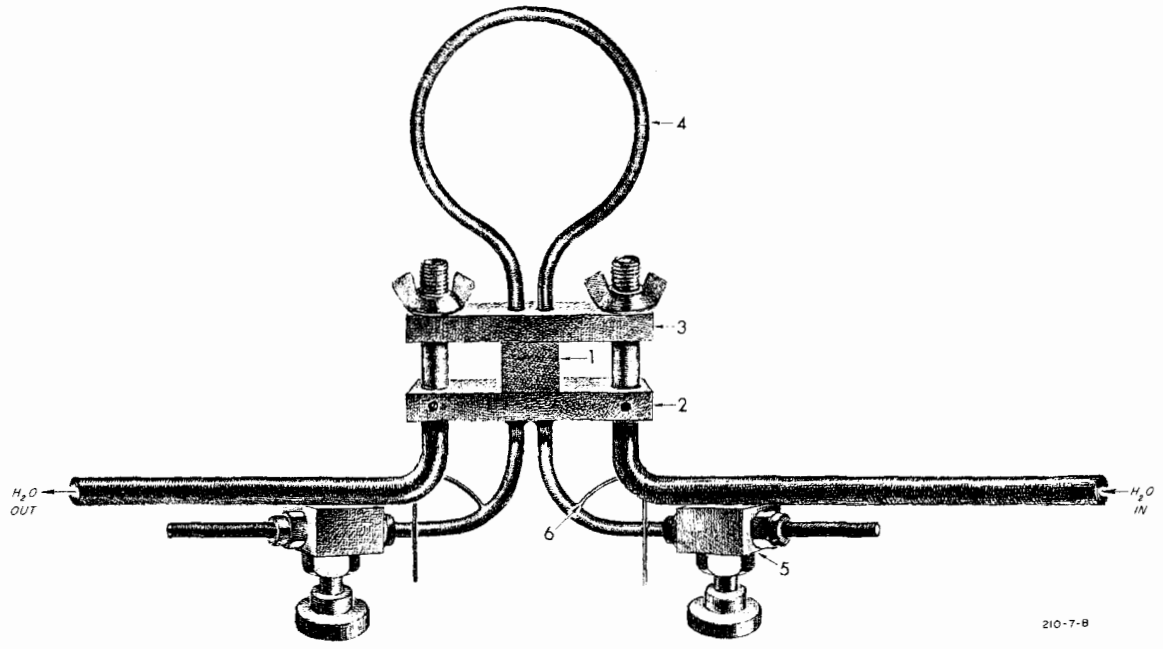

FIG. 9--Detail design of the sample holder: (1) sample; (2) fixed clamping bar; (3) movable clamping bar; (4) water cooling copper tubes; (5) needle valves; (6) thermocouples.

3. The conductors were wrapped individually with glass fiber tape as described in (2). In addition to the individual conductor insulation, both conductors were wrapped in glass fiber tape (half-overlapped) (Fig. 8c).
4. The tape used for conductor insulation [as in paragraphs (2) and (3)] was a B-staged epoxy combined with glass tape. The sample was wrapped in mylar. Pressure was applied to it by means of flat plates during curing.
5. The tape used for conductor insulation [as in paragraphs (2) and (3)] was glass fiber cloth and micafleece with approximately 7.5-10% organic binder.
6. The tape used for conductor insulation [as in paragraphs (2) and (3)] was glass fiber, medium weave, and the conductor insulation to ground was B-staged epoxy in combination with micafleece.

The different epoxy resins used for radiation tests and the curing agents are discussed below.

1. DER 332 and DER 332 LC* and DEN 438

DER 332 is a diglycidyl ether of bisphenol A with an epoxide equivalent of 175. Because of its high purity (it contains practically no aliphatic chains and its chlorine content in the glycidyl ether is low), it assures uniform performance and low viscosity and has very good mechanical, electrical, and radiation properties.

DER 332 frequently crystallizes at room temperature. Warming to 60-70°C restores the resin to a liquid state. DER 332 LC (low chlorine) is extremely pure and has excellent radiation properties. Its structure in simplified form is:

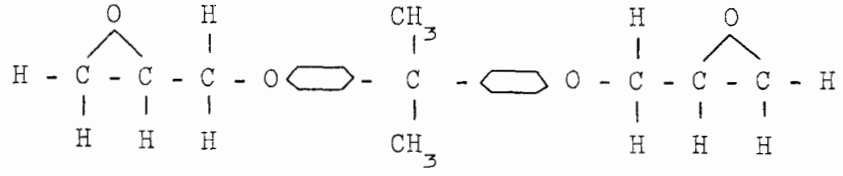

A mixture of DEN 438/DER 332 with an aromatic curing agent will give a charred composite with two to three times the strength of DER 332 char alone. DEN 438 has a high viscosity, but the blend of DEN 438/DER 332

*Dow Chemical Company, Freeport, Texas.

with a 1/3 parts per weight ratio has low viscosity and gives a high char strength. DER 332 was used in combination with the following curing agents:

a. BF_3MEA* [boron trifuluoride mono ethyl amine complex $BF_3(C_2H_5NH_2)$] is classed as a Lewis acid. The BF_3 content is 61%. Three parts per weight of BF_3MEA were used per hundred parts of epoxy resin DER 332. The two-stage curing process consisted of precuring at 80°C for four hours, then postcuring at 160°C for twelve hours. BF_3MEA contains an aliphatic amine, but was used because of its unique features, such as long pot life (at room temperature, several days) and high heat distortion temperature (149-180°C). These features allow it to be used with a large number of different epoxies. It also has good chemical resistance and good electrical properties. Figure 10 shows the viscosity of DER 332 with BF_3MEA as a function of temperature.

The BF_3MEA epoxy resin system cures on breakdown of the BF_3 complex, which begins to be significant in rate at about 80°C.

When exposed to radiation, both the acid and basic fragments of the curing agent start to show gas evolution at room temperature. The presence of these fragments in the cured casting would give built-in degradation sites when the sample was exposed to a high irradiation dose rate. A BF_3MEA level of <u>one</u> part per weight of epoxy may greatly extend the life of the binder on irradiation but requires a longer initial cure cycle. Mechanical and electrical tests with the BF_3MEA epoxy resin system (DER 332) with 50 parts per weight of alumina filler epoxy show complete degradation at radiation dosages exceeding 10^{13} ergs gr^{-1}.

b. Epon resin curing agent Z** is a modified aromatic polyamine. It contains approximately 50 parts per weight of the total curing agent metaphenylene diamine. The system cures by stoichiometric reaction

---

*Harshaw Chemical Corporation, Shell Chemical Corporation as Epon curing agent BF_3-400.

**Shell Chemical Corporation.

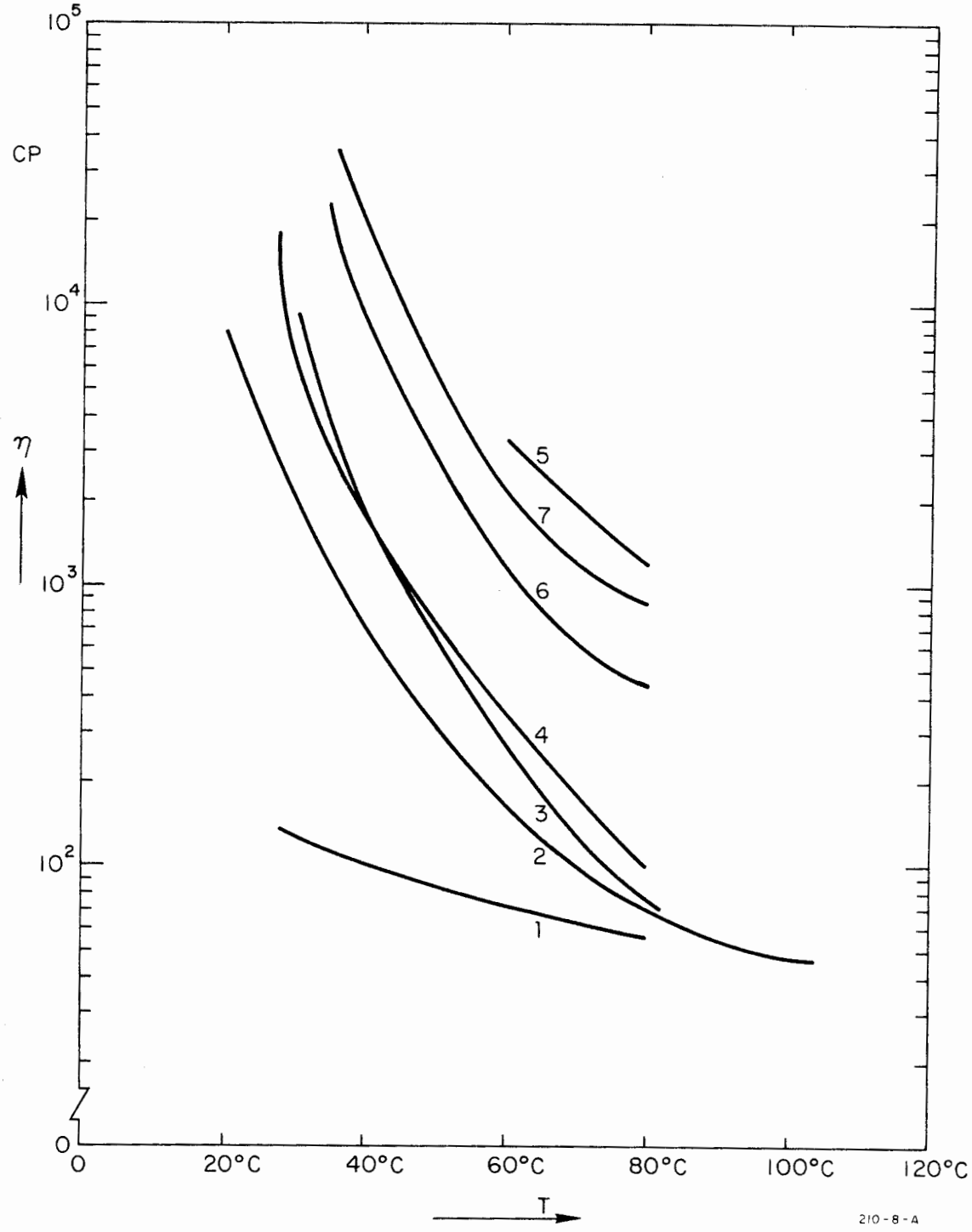

FIG. 10--Viscosity of different thermosettings as a function of temperature. (1) Dow Corning low pressure silicone R-7521; (2) DER 332 LC (Dow Chemical Company); (3) DER 332 and BF_3MEA; (4) Epon 828 (Shell Chemical Corporation; (5) DER 332 and BF_3MEA filled with alumina (100 p.p.w. of DER 332); (6) DER 332 LC and MPDA, DMA hardener filled with alumina (100 p.p.w. of DER 332 LC) and thixotropic material (Cab-o-sil 1 p.p.w. of DER 332 LC); (7) DER 332 LC and MPDA, DMA hardener filled with alumina (120 p.p.w. of DER 332 LC) and (1 p.p.w. of DER LC) Cab-o-sil.

between the amine and the epoxy resin until all primary and secondary amine hydrogens are used up, at which point the amine still has the potential of curing epoxy catalytically as a tertiary amine. Seventeen to nineteen parts per weight of Epon Z were used per hundred parts of DER 332. Epon Z is liquid. It may form crystals if stored at room temperature, but slight warming prior to use produces clear liquid. DER 332 and Epon Z have low viscosity at casting temperature (Fig. 10). Epon Z has excellent chemical resistance and high heat distortion temperature. A drawback is the moderate, but sufficiently long, pot life of only three hours at 45°C and eight hours at 25°C.

Small castings are precured at 80°C for two hours and postcured at 150°C for two hours. Large castings should be gelled at room temperature and cured at 80°C-100°C for twelve hours.

c. In order to achieve the highest possible radiation resistance, a mixture of very pure metaphenylene diamine (MPDH)* and methylenedianiline (MDA)** was used as the curing agent for DER 332 LC

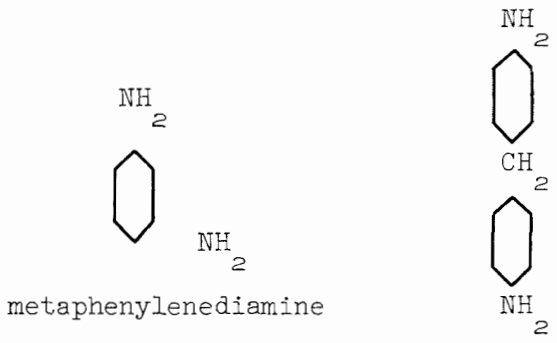

metaphenylenediamine

methylenedianiline

The mixture ratio of metaphenylenediamine (MPDA) to methylenedianiline (MDA) is 40:60 parts per weight. Eighteen to nineteen parts per weight of this curing agent were used per hundred parts of DER 332. The mixture should be prepared at 60-65°C. The viscosity curve of the mixture as a function of temperature follows the curve of DER 332 and Epon Z. At 68°C the viscosity of the epoxy system was measured to be

---

* E.I. Du Pont de Nemours and Co.

** Dow Chemical Company.

approximately 55 cP. The pot life of DER 332 with the mixture of meta-phenylenediamine and methylenedianiline is about four hours at 45°C and 10 hours at 25°C.

The aromatic amine plasticizes the mixture, making possible higher filler loading. The hardener decreases the viscosity of the mixtures compared with the initial resin viscosity given in curve 2 of Fig. 10. An alumina filler loading of 120 parts per weight of the epoxy hardener system had a viscosity of approximately 850 cP at 60°C. (The addition of 1 part per weight of Cab-o-sil to the epoxy system increased the viscosity to approximately 920 cP.)

2. Epon 828 and 1031*

A casting and impregnation solution of low viscosity (Fig. 10) and good handling properties is obtained by using a mixture of Epon 1031 and 828 with a ratio of 1:1. The mixture has a heat distortion temperature of 197°C and a room temperature compressive strength of 1450 kg/cm^2. Epon 1031 is a solid resin with high functionality and reactivity. It consists of a mixture of isomers and homologues having the structure

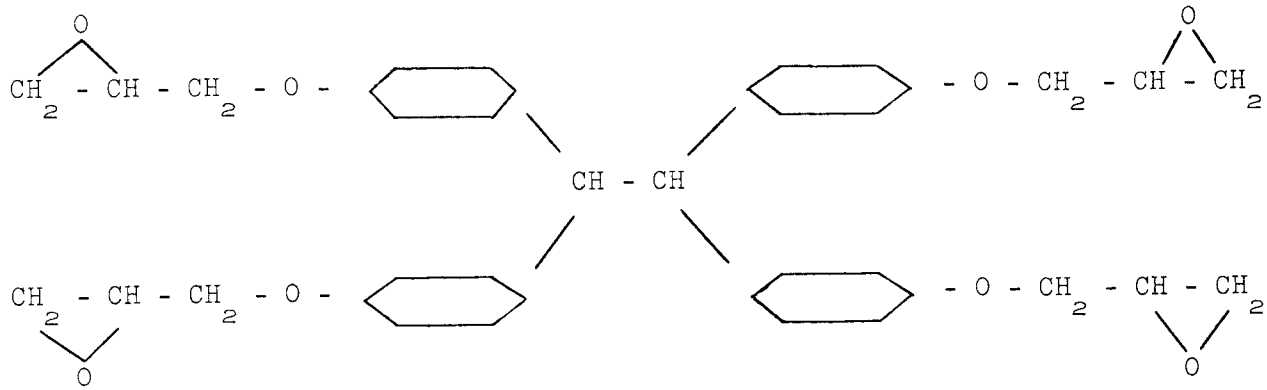

Due to difficult handling properties and high viscosity Epon 1031 is blended with Epon 828.**

Epon 828 is a light colored, epichorohydrin/bisphenol, A type, low molecular weight epoxy resin. The chemical structure of a typical Epon 828 molecule is:

---

*Shell Chemical Corporation.

**Shell Chemical Corporation.

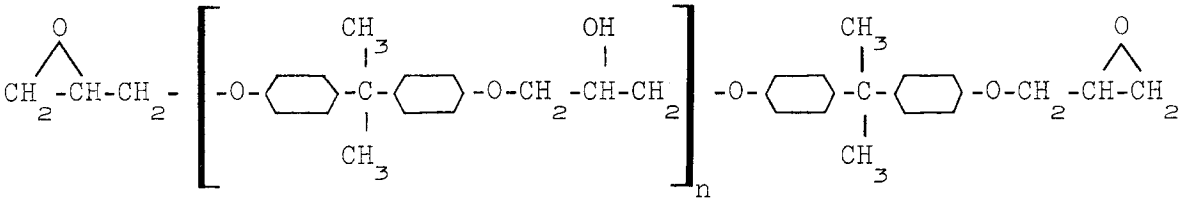

with $n \approx 0.1$.

The viscosity as a function of temperature is given in Fig. 10. Epon 828 has fewer epoxy groups per mole than DER 332 and has an epoxide equivalent weight of 185-192. Due to the presence of aliphatic chains in the complex, the radiation resistance of 828 is somewhat lower than DER 332.

The aromatic curing agent used with Epon 1031/Epon 828 was a mixture of nadic methylanhydride (NMA) and benzyl dimethylamine (BDMA).* NMA, with a concentration of 80 parts per weight, and BDMA, with a concentration of 0.5-1 part per weight of Epon 828/Epon 1031, were used as catalyst and accelerator. Pot life at room temperature was 10-12 hours. Initial curing was done at 60°C for 2-4 hours; postcuring was done at 150°C for 4-6 hours.

3. Stycast 2850 FT**

Stycast 2850 FT is a modified and mineral-filled diglycidyl ether of bisphenol A with an epoxide equivalent weight of approximately 190. It has very little chlorine content in side chains and a high heat distortion temperature of 175°C. It is commercially available with an alumina filler. The alumina content is approximately 130-140 parts per weight of 2850 FT. Due to the high viscosity of the system, Stycast 2850 FT can be used as a casting resin or for wet-winding. Heating it up to 40°C reduces the viscosity to 12,000 cP. At 60°C its viscosity is still higher than 8000 cP. The curing agent to be used with Stycast 2850 FT is catalyst 11 with approximately 4 parts per weight of the resin. Catalyst 11 is an aromatic amine eutectic with metaphenylene diamine as the major component.

---

*Shell Chemical Corporation.

**Emerson and Cuming Inc., Canton, Mass.

Stycast 2850 FT has a pot life of approximately 1.5 hours. Other epoxies similar to 2850 FT which have been tested are Eccoseal 1207 and Eccoseal W19.

4. Eccoseal 1207*

Eccoseal 1207 has excellent high temperature features. It can be used continuously up to 177°C. The curing agent is built in the epoxy system. In order to accelerate the curing, an accelerator (catalyst 20) with a concentration of 15 parts per weight of the system is used. Catalyst 20 is a modified aliphatic amine. Eccoseal 1207 has a viscosity of 150 cP at 60°C. The radiation properties of 1207 filled with alumina, 100 parts per weight of the resin system, are comparable to stycast 2850 FT.

5. Eccoseal W19*

The basic resin system of Eccoseal W19 is slightly different from stycast 2850 FT. It is used in combination with catalyst 11. Sixteen to eighteen parts per weight of catalyst are used with W19. The viscosity of a W19 system at 60°C is approximately 120 cP; it may be filled with a mineral filler and has radiation properties similar to Epon 828 and curing agent Z.

6. Silicone Resin R-7521**

From different silicones we chose silicone R-7521 resin, which combines a number of features that make it valuable for coil insulation.

At room temperature R-7521 has a viscosity of 135 cP, which decreases to about 80 cP at 60°C.

Filled and glass fiber reinforced R-7521 (cured) is hard and has a compression strength of approximately 1600 kg/cm^2. R-7521 is mixed with recrystallized dicumyl peroxide*** as the curing agent. The proportions are 1.5 parts per weight hardener to 100 parts per weight of R-7521, and 0.25 parts per weight accelerator N, dimethyl-p-toluidine, to 100 parts per weight of R-7521. R-7521 is filled with 900 parts of zirconium ortho

---

*Emerson and Cuming, Inc., Canton, Mass.

**Dow Corning Corporation, Midland, Michigan.

***Wallace A. Erickson and Co., Chicago.

silicate (Ultrox),* 15-20 microns grain size. The resin and filler may be supplied in the preparation of 100 to 900 parts per weight, or the amount of filler desired may be mixed to the resin.

The pot life at 60°C is greater than two weeks.

The curing process takes six hours at 150°C; then five hours at 250°C. R-7521 cures without evolution of volatile materials.

The differences in radiation resistance between different epoxies and curing agents may be described briefly as follows. Degradation of epoxies occurs when covalent bonds in molecular structure are broken. Chemical changes happen because of double bond formation, cross-linking oxidative degradation, polymerization and depolymerization, and gas evolution. Degradation can be decelerated by minimizing radiation sensitive impurities in the system. This may be one explanation for the slight difference in radiation resistance of DER 332 LC cured with MDA and MPDA and Epon 828 cured with Epon Z. Another explanation may be found in the difference of the equivalent ratio between epoxy and hardener. An excess of epoxy is good because the epoxy resin is more stable to radiation than the hardener. Also, a certain excess of epoxy stabilizes the system to radiation by scavenging some degradation products. At a fixed hardener weight, a DER 332 mix (EEW 175) contains more epoxy than would Epon 828 (EEW 192). The choice of the proper epoxy hardener system is dictated, of course, not only by the high radiation resistance of the system, but also by ease in manufacturing, compatibility to the fillers, and pourability.

7. Mineral Fillers

The effect of mineral fillers on mechanical and electrical properties and radiation resistance was discussed previously. Among a vast variety of inorganic fillers, we were able to investigate the functional effects of only a few materials. The materials which seemed of primary interest were aluminum oxide, ground glass, magnesium oxide, mica, and silica. The chosen particle size for the above fillers was 10-20 microns, equivalent to a mesh size 900. The above-mentioned fillers are readily

---

*Orefraction Mineral Products, distributor: M & T Chemical Inc., Rahway, N.J.

available commercially and their properties are given in Table IX. The ability of a filler to stay in suspension is related to its particle size and shape, its inherent density, the viscosity of the filled impregnant, and the pH of the system. Most fillers with 900 mesh size stay in suspension without the addition of thixotropic materials. However, as a further safeguard, a colloidal silica such as Cab-o-sil* (1-3 parts per weight of the weight of the resin) was added to the system, which increases the viscosity slightly, but keeps the filler in suspension. It may be emphasized that the addition of mineral fillers to thermosettings (such as epoxies) reduces their mechanical strength. The addition of Dow Corning Z-6040** to the filler or to the resin system improves the mechanical strength of the resin system. The addition of Z-6040 in a concentration of 1-2 parts per weight of the epoxy improves the mechanical strength of mineral-filled (silica) castings, giving tensile strength in excess of that for unfilled systems. This is presumed to be due to better wetting of the filler and easier elimination of air in mixings.

Optimum results, concerning mechanical and thermal properties and radiation resistance, were achieved by choosing the amount of filler to be 100-120 parts, and Z-6040 1-2 parts per 100 parts by weight of the epoxy.*** The filled resin should still have a viscosity less than 2000 cP to guarantee a uniform void-free impregnation. In Fig. 10 the viscosity of Al_2O_3-filled DER 332 and the MPDA, MDA system is given as a function of temperature. No thixotropic components are added to the resin; the amount of Al_2O_3 was 100 parts per weight of DER 332. The addition of Cab-o-sil, 1 part per weight of the epoxy, increased the viscosity of the system at 60°C by about 70 cP.

---

*Trade name, Godfrey L. Cabot, Inc.

**Z-6040 is Dow Corning's tradename for an epoxy-functional material, glycidoxyl-propyl trimethoxy silane, used as a finish to glass fabrics and to mineral fillers, as an additive to prepare the resin-glass-filler structure. It operates as a wetting agent and provides high strength to the structure.

***In further notations the weights of corresponding additive to the main thermoset, i.e., epoxy is mentioned simply as per weight of the epoxy which means that to 100 parts of Epoxy (per weight) x parts of filler, or hardener etc. is added.

TABLE IX

INORGANIC FILLERS AND THEIR PROPERTIES

Filler	Molecular Composition	Description	Particle Size Sieve Fineness	Specific Density gr cm^{-3}	Thermal Conductivity $W/cm^{o}C$	Melting Temperature ^{o}C	Type of Particle
aluminum oxide	Al_2O_3 (99%)	alumina	900 mesh	3.7-3.9	9×10^{-4}	> 1700	white plate-shaped crystals
ground glass	silica 66.9% CaO 10.5% MgO 2.2%	milled glass cullet	900 mesh	2.5	3.12×10^{-5}	1500	fine powder white
magnesium oxide	MgO 98% CaO 1% SiO_2 0.5%		900 mesh	3.5-3.7	7.8×10^{-6}	2800	fine gray powder
mica	SiO_2 45.2% Al_2O_3 38.5% K_2O 11.8%	water ground muscovite	1000 mesh	2.8-3.1	3.1×10^{-5}	1500	off-white thin plates
silica	SiO_2 99.5%	amorphus silica	900 mesh	2.65	3×10^{-5}	~ 1300	soft ultrafine quartz

IV. RADIATION EFFECTS ON COIL INSULATIONS

The samples (Fig. 8) were chosen so as to reduce the insulation damage due to thermal neutrons to a minimum. The continuous control and recording of the inlet and outlet water temperature during irradiation from the Mark IV electron linear accelerator guarantee that the sample temperature rise is kept within boundaries, which may also be expected in magnet operation. The water temperature rise did not exceed 25°C throughout the test, and the maximum temperature at the insulation surface was below 72°C at the shower peak. Irradiated samples at the University of California (Livermore pool type) reactor were immersed in tap water during the radiation period and the sample temperature was checked and recorded closely so that it did not exceed 100°C.

The absorbed power from electrons corresponds to a maximum of 700 watts (data obtained at Stanford's Mark IV accelerator with 60-70 MeV beam energy, 360 pulses per second repetition rate, 16-30 microamps average current).

From the temperature rise in the water and the weight of the sample (15 grams), the absorbed flux was determined to be 4.65×10^8 ergs/gr, corresponding to 30% of the maximum beam power.

The location of the samples in the test area between the linear accelerator and the Faraday cup is seen in Fig. 11. The white spot in the sample shows the beam effect of the bombardment. The electron passes one insulation layer between conductors and part of both water-cooled conductors.

Tests performed at the Mark IV accelerator with different samples were:

1. Determination of mechanical properties as a function of absorbed radiation dose. The tests were limited in evaluation to the relative bonding strength of the thermosetting to the conductor, the impact strength, and the compression strength.
2. Determination of the electrical properties as a function of absorbed radiation dose. The relative insulation resistivity of the dry and wet samples and the insulation strength in (volts/cm) were evaluated.

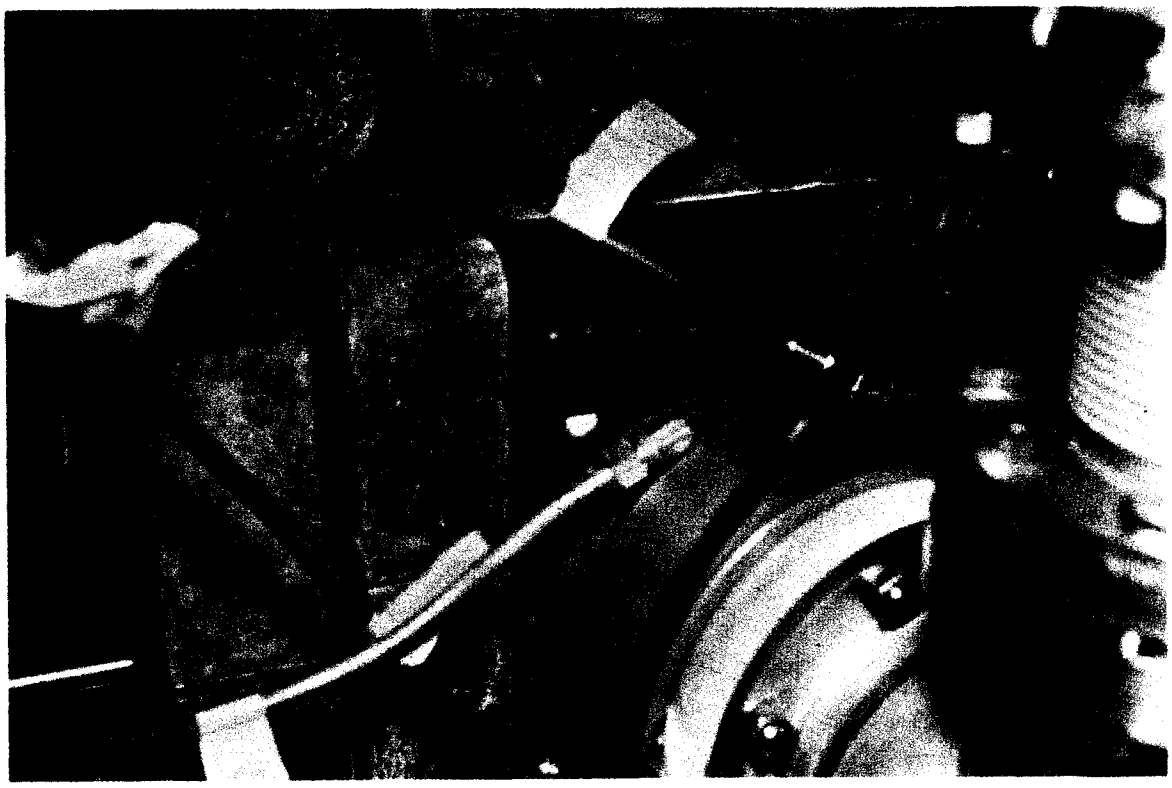

FIG. 11--Location of the irradiated sample in the experimental area of the SLAC Mark IV. Part of the accelerator is visible in front. The irradiated sample and part of the sample holder are seen in the background. The white spot is due to irradiation with the electron beam.

3. Determination of moisture absorption as a function of absorbed radiation dose. Because of the required high absorbed radiation dose (10^{13}-10^{15} ergs·gr^{-1}), the samples had to be irradiated over a long period of time and it was difficult to evaluate the data on a large number of samples to determine the average values. Tests performed were carried out during parts of 1963 and 1964. The test data given in the next section are averages from 3-5 samples built and insulated in the same manner with the same organic thermosettings.

The insulations tested were:

a) DER 332 LC and catalyst MPDA, MDA with an Al_2O_3 filler 100-120 parts per weight of the DER 332 LC hardener system and Cab-o-sil 1 part per weight of the epoxy.*

b) Stycast 2850 FT and catalyst 11.

c) Glass fiber reinforced DER 332 and BF_3MEA, unfilled, and filled with Al_2O_3 900-mesh in a concentration of 100-120 parts per weight of the epoxy system (Cab-o-sil 1 part per weight of epoxy).

d) Glass fiber reinforced DER 332 LC and Epon Z, filled with Al_2O_3 900-mesh 100 parts per weight of DER 332 LC hardener system.

e) Glass fiber reinforced DER 332 LC and catalyst MPDA, MDA with Al_2O_3 filler 120 parts per weight of the resin system (Cab-o-sil 1 part per weight of epoxy).

f) Glass fiber reinforced mixture of Epon 828 and 1031, filled with Al_2O_3 900-mesh 100 parts per weight of 828/1031.

g) Glass fiber reinforced stycast 2850 FT and catalyst 11, filled with Alumina filler 130 parts per weight of stycast 2850 FT.

h) Glass fiber reinforced Eccoseal W19 and catalyst 11, filled with Al_2O_3 900-mesh 100 parts per weight of Eccoseal W19 (Cab-O-sil 1 part per weight of W19).

i) Glass filler reinforced R-7521 silicone and catalyst dicumyl peroxide filler with zircon (zirconium ortho silicate) 900 parts per weight of R-7521.

j) Glass fiber reinforced Eccoceram 21, part A and part B.

*In this and further information see page 48.

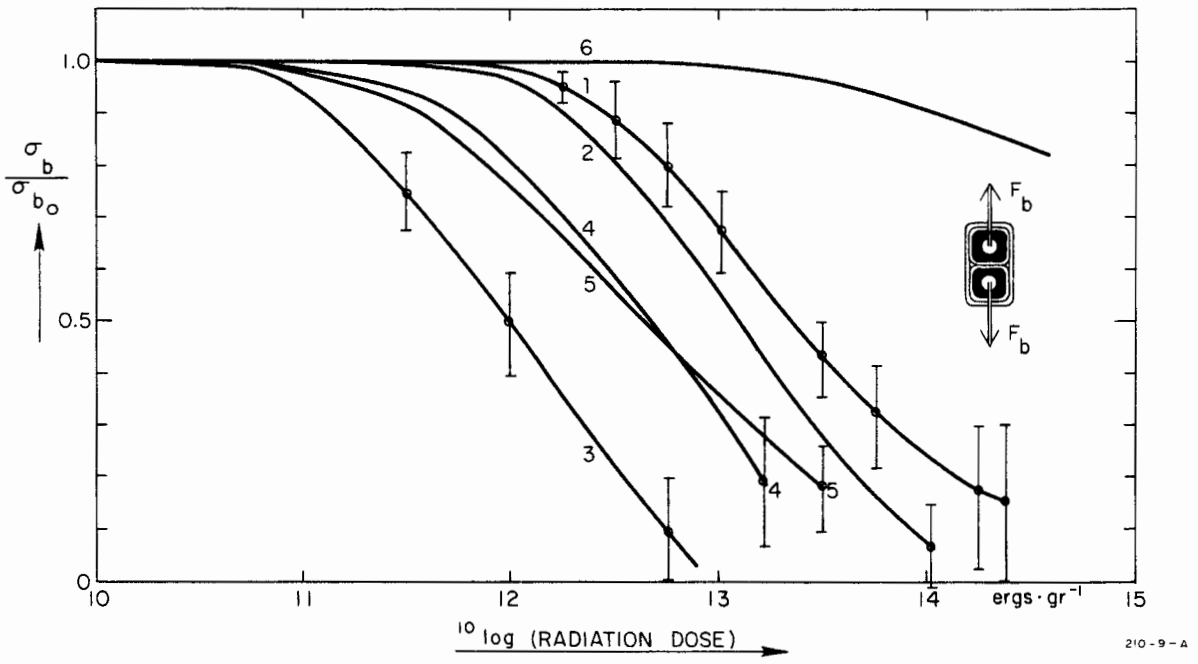

FIG. 12--Bond strength of glass fiber reinforced and mineral-filled thermosettings and ceramica. (1) DER 332 LC and curing agent MPDA and MDA wetting agent Z6040 (σ_{b_i} = 183 kg cm^{-2}); (2) Epon 828/1031 curing agent NMA and BDMA (σ_{b_i} = 189 kg/cm^2); (3) Emerson and Cuming 2850 FT no glass fiber reinforcement (σ_{b_i} = 62 kg cm^{-2}); (4) DER 332 LC and curing agent BF_3MEA (σ_{b_i} = 175 kg cm^{-2}); (5) Dow Corning R-7521 silicone and curing agent dicumyl peroxide; zircon filler (σ_{b_i} = 70 kg cm^{-2}); (6) Eccoceram part A and B (σ_{b_i} = 22 kg cm^{-2}).

A. Mechanical Properties

1. Bond Strength

The bond strength did not change appreciably up to the absorbed radiation dose of 9×10^{10} ergs·gr^{-1}. Above this dose the bond strength of different thermosetting systems changed, as shown in Fig. 12. The initial values of bond strength for different thermosettings measured are given below.

Filled thermosettings: 62 kg·cm^{-2},
Laminated filled epoxies: 183 kg·cm^{-2},
Laminated filled silicone: ≈70 kg·cm^{-2},
Laminated ceramics: 22 kg·cm^{-2}.

These values appear to be low compared to data given in the literature. It may be pointed out that fractions of the surfaces between the two conductors were probably not bound properly. With samples illustrated in Figs. 8 and 9, it is difficult to guarantee a complete uniform bonding. The copper conductors obtained were not perfectly straight, which added to the difficulties; however, it should be mentioned that ideal conditions cannot be found in magnet coil manufacturing, either. We believe, therefore, that the given bond strength values represent true coil manufacturing conditions.

At a dose of 1.1×10^{14} ergs·gr^{-1}, epoxy DER 332 LC and curing agent MPDA and MDA, with Al_2O_3 filler 50 parts per weight of DER 332 LC, had a bond strength of 58 kg·cm^{-2}. This value is still higher than the bond strength of Eccoceram, which changed its relative bond strength to 0.86 of its initial value.

At a dose of 3.25×10^{14} ergs·gr^{-1}, the bond strength of DER 332 with the catalyst MPDA and MDA was reduced to 20.3 kg·cm^{-2}.

2. Compression Strength

Laminated DER 332 LC and Al_2O_3 and curing agent MPDA and MDA show an increase of compression strength up to the radiation dose of 3.6×10^{11} ergs·gr^{-1}. At higher absorbed irradiation doses, the compression strength changed according to curve 1 in Fig. 13. Other epoxies and glass fiber laminates follow the same features as measured for DER 332 LC. The initial value of compression strength at zero radiation dose and 25°C was measured to be 3250 kg·cm^{-2}.

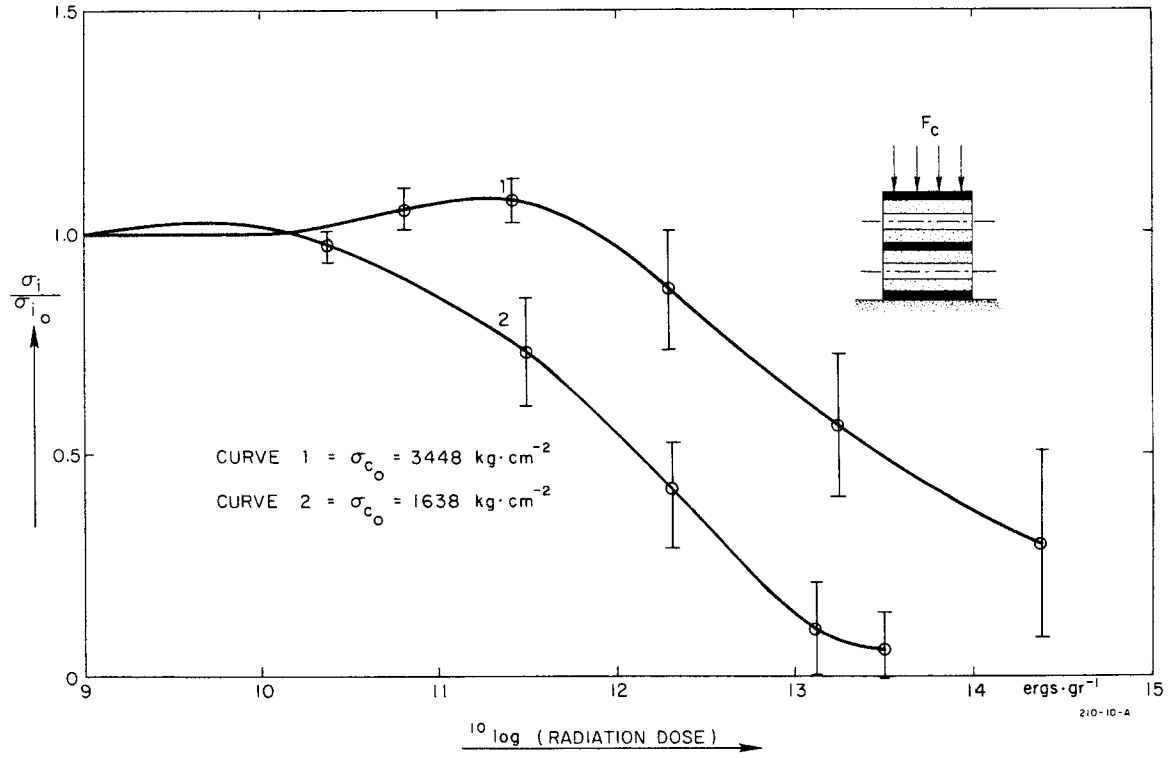

FIG. 13--Relative compression strength of glass fiber reinforced, mineral-filled thermosettings as a function of absorbed radiation dose. (1) DER 332 LC and hardener MPDA and MDA (Al_2O_3 filler); (2) R-7521 silicone resin hardener dicumyl peroxide (zir

3. Impact strength

The evaluation of the impact strength of thermosettings as a function of the absorbed irradiation dose was somewhat difficult owing to irregularities of the insulation thickness. The insulation thickness between the copper conductors could be determined only very crudely by measuring the visible insulation thickness at the two conductor end surfaces. The deviation of the insulation thickness inside the two conductors was not considered in the test evaluation. The standard impact strength specimen could not be used because of the heating problems during radiation explained previously. In Fig. 14 is shown the relative impact strength of Al_2O_3-filled DER 332 LC, which was measured with the Baldwin pendulum cantilever beam impact testing machine of Izod type. The impact strength is the breaking energy in kg·cm divided by the thickness of the insulation in cm between the two bonded conductors. The relative impact strength changed to 0.76 when exposed to the absorbed radiation dose of 4.9×10^{12} ergs·gr^{-1}. No appreciable changes could be measured up to 2.4×10^{11} ergs·gr^{-1}. After exposure to a radiation dose of 3.2×10^{14}, the impact strength of the samples was practically zero.

B. Electrical Properties

1. Volume Resistivity

The insulation resistance between the two water-cooled conductors was measured with a high megohm bridge. The insulation resistance was measured intermittently after interrupting the radiation of the sample. The insulating sheet between the two conductors had a surface area of $2.6 \times 1.2 = 3.12$ cm and an insulation thickness of 0.08 cm.

The upper limit of the bridge is 1.5×10^{13} ohms. Prior to irradiation, the insulation resistance of dry insulation at the 500-volt level was measured to be 1.5×10^{13} ohms, which gives a volume resistivity of at least

$$1.5 \times 10^{13} \times 3.12/0.08 = 5.86 \times 10^{14} \text{ ohms·cm.}$$

The change in volume resistivity as a function of absorbed radiation dose is given in curve 1 of Fig. 15 for glass fiber reinforced and Al_2O_3-filled DER 332 LC. The volume resistivity had changed at the absorbed radiation dose of 1.1×10^{14} ergs·gr^{-1} to 1.755×10^{11} ohms·cm and at a dose of 3.25×10^{14} ergs·gr^{-1} to 7.8×10^{10} ohms·cm.

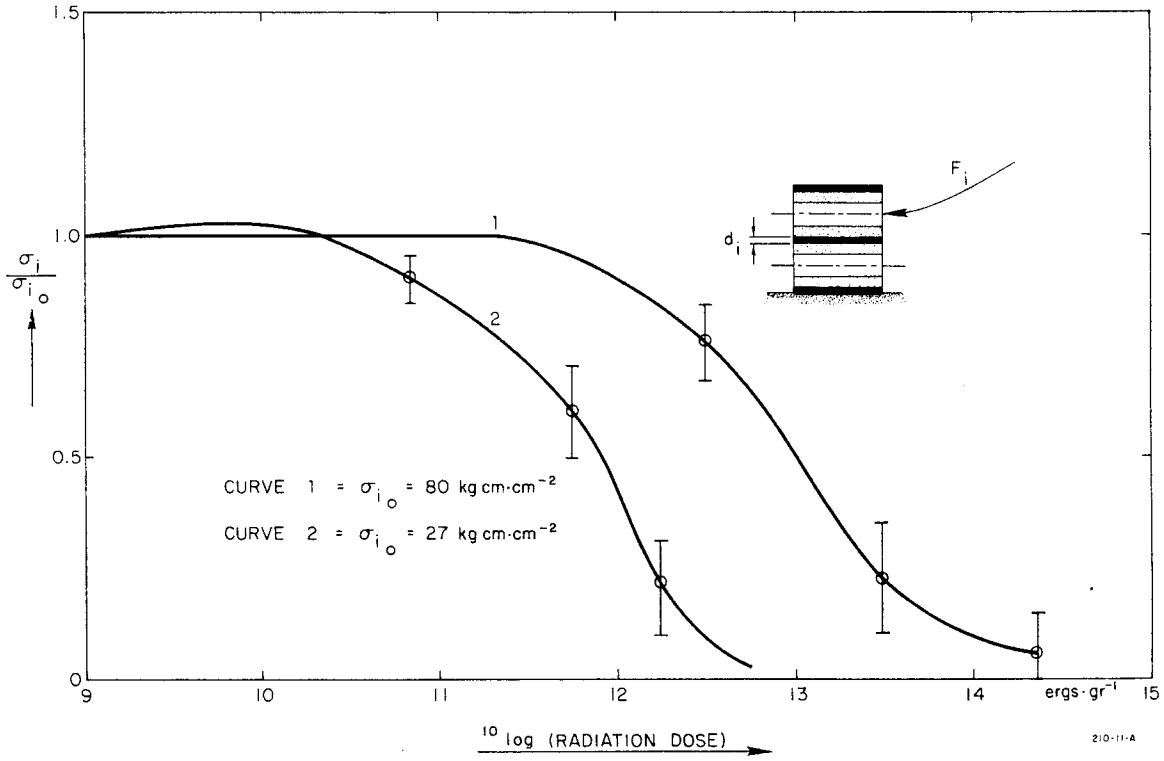

FIG. 14--Relative impact strength of glass fiber reinforced, mineral-filled thermosettings as a function of absorbed radiation dose. (DER 332 LC and MPDA and MDA (Al_2O_3 filler); (2) R-7521 silicone resin (zircon filler).

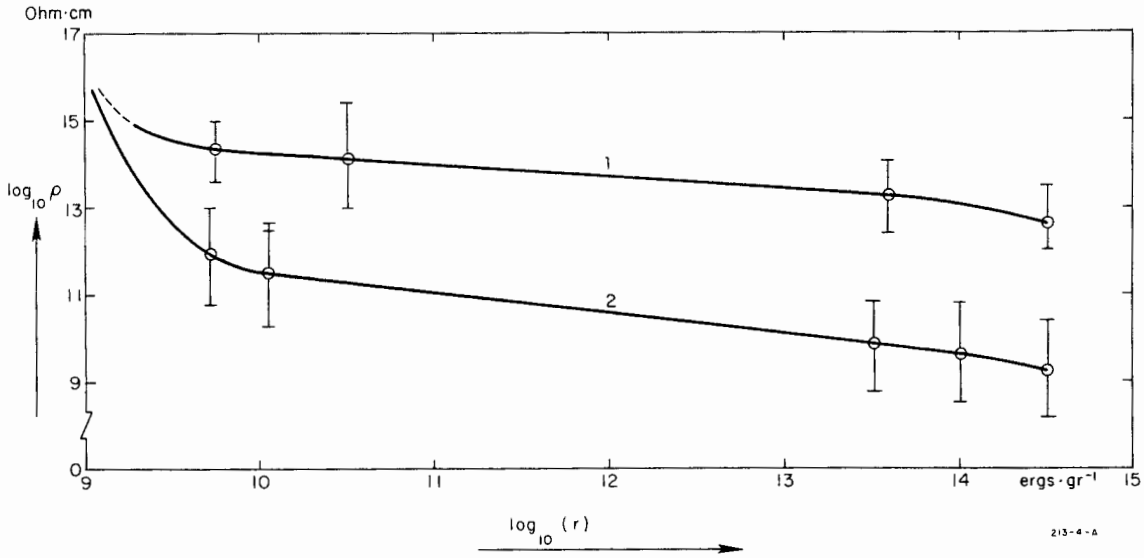

FIG. 15--Volume resistivity of glass fiber reinforced, mineral-filled thermosettings as a function of absorbed radiation dose. (1) DER 332 LC hardener MPDA and MDA (Al_2O_3) filler; (2) R-7521 silicone resin hardener dicumyl peroxide (zircon filler).

The volume resistivity of water-immersed epoxy, glass laminate samples, is shown in Fig. 4. The volume resistivity of water-immersed insulations as a function of absorbed irradiation dose is given in curve 2 of Fig. 15. Samples had been immersed in tap water at room temperature 24 hours after each irradiation. Moisture repellant organic coatings and films are readily destroyed at approximately 10^{12} ergs·gr^{-1} absorbed dose, and irradiated glass fiber reinforced thermosettings shows greater affinity toward moisture and water absorption. Repeated drying leads to an increase of volume resistivity but does not improve the mechanical properties of the irradiated samples. Coils in a radiation environment should be kept dry if possible and all provisions should be made to keep the insulations from permanent wetting.

It may be pointed out that even when the mechanical properties of insulations are degraded, the insulation resistivity of dry insulations is still satisfactory.

Continuous application of 500 volts on the samples during radiation did not essentially demonstrate a difference in insulation resistance, as can be seen from curves 1 and 2 of Fig. 16a. The insulation resistance drops by a factor of 10^2 at the absorbed radiation level of 8.2×10^{10} ergs·gr^{-1}, and continues to decrease at a slower pace up to the highest measured radiation dose of 3.25×10^{14} ergs·gr^{-1}, where it is 8×10^{10} ohm·cm. Test sample and the test equipment are shown in Fig. 16b.

2. Dielectric Strength

A 15,000-volt 60-CPS, SLAC-made corona measuring device, shown in Fig. 17a and 17b, was used to determine the corona threshold values as a function of absorbed radiation dose. Rogovsky electrodes (0.5-inch-diameter) were used for testing. One electrode was stationary and the other electrode could be adjusted by spring loading to the required pressure. The conductor was grounded and the applied voltage was raised in increments of 50 volts until breakdown. Corona threshold, discharge level, and breakdown voltages were recorded. The voltage was kept between two voltage steps for 30 seconds. Figure 18 illustrates the corona threshold and dielectric strength of glass fiber reinforced, Al_2O_3-filled DER332LC and Epon 828/1031. No significant difference was observed between the different reinforced and filled epoxies cured with aromatic curing agents.

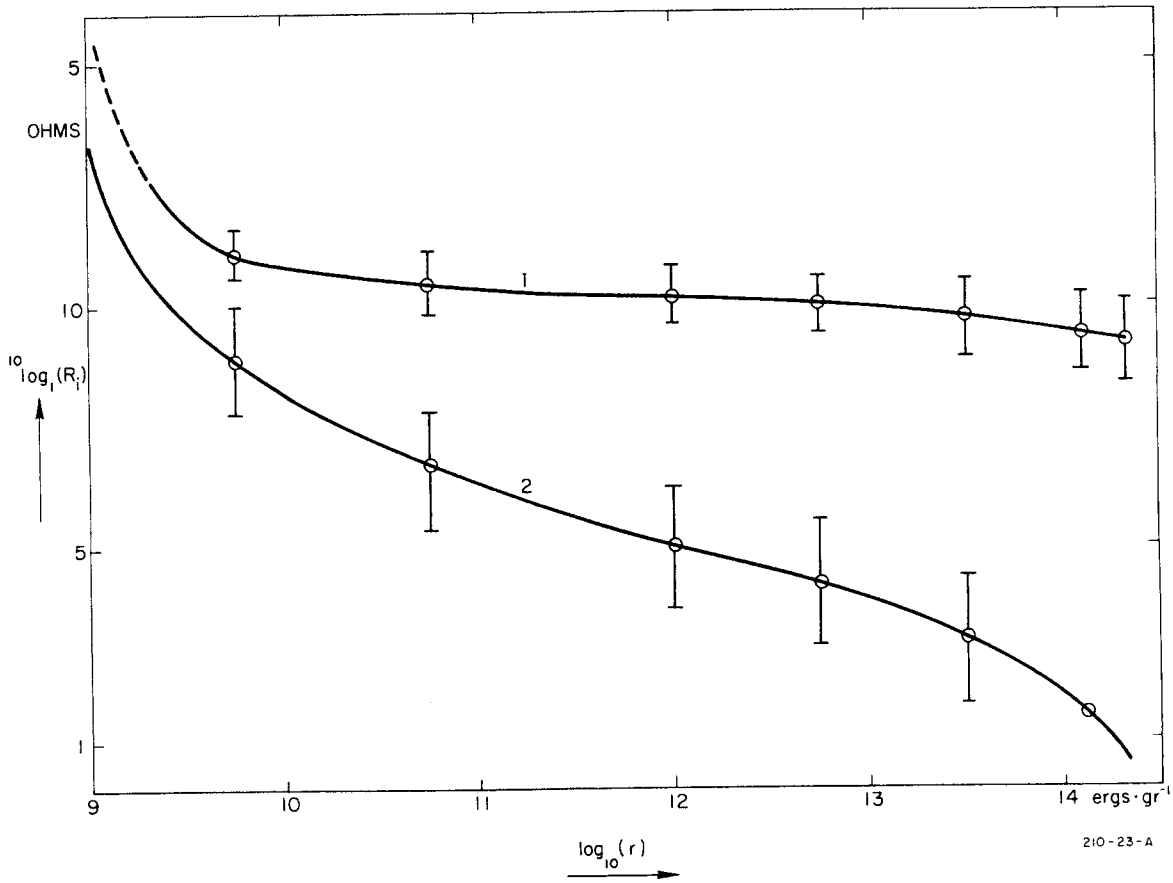

FIG. 16a--Insulation resistance of irradiated glass reinforced thermoset according to the following specifications:
Epoxy DER 332 LC hardener MPDA and MDA
Alumina filled and glass reinforced with glass tape
Volan A treated medium weave
Curve 1 dry insulation; curve 2 wetted insulation

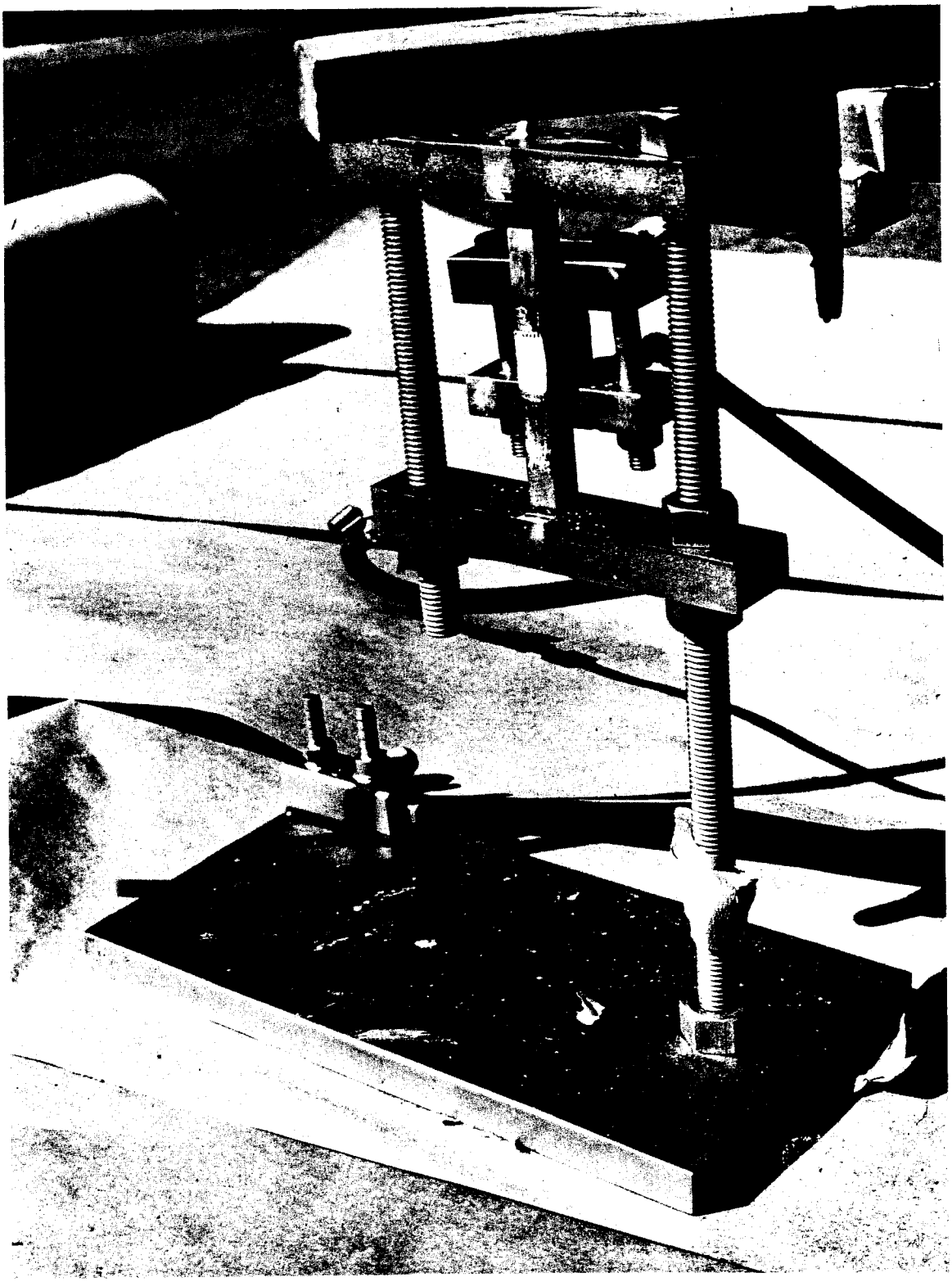

FIG. 16b--Sample and sample holder for dielectric test measurement.

FIG. 17a--Test equipment for measurement of the corona threshold of irradiated samples. The sample holder is visible at the right.

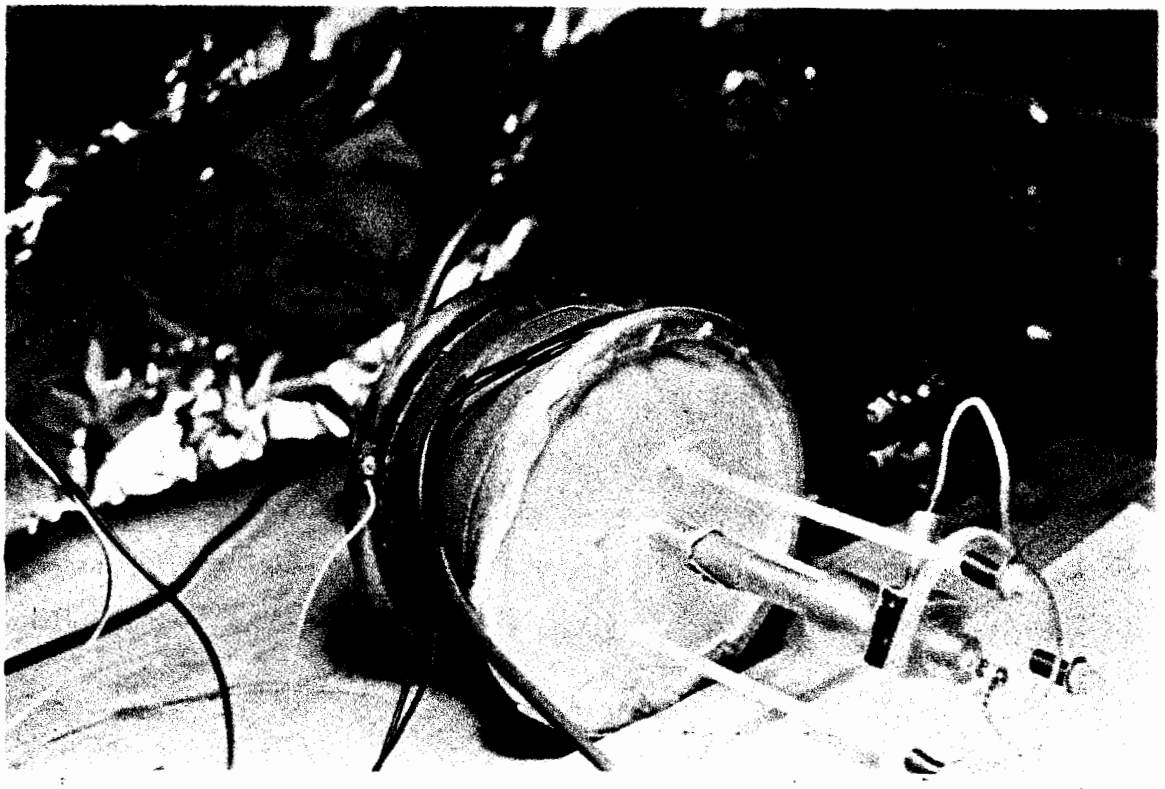

FIG. 17b--Sample holder and sample for the measurement of corona threshold.

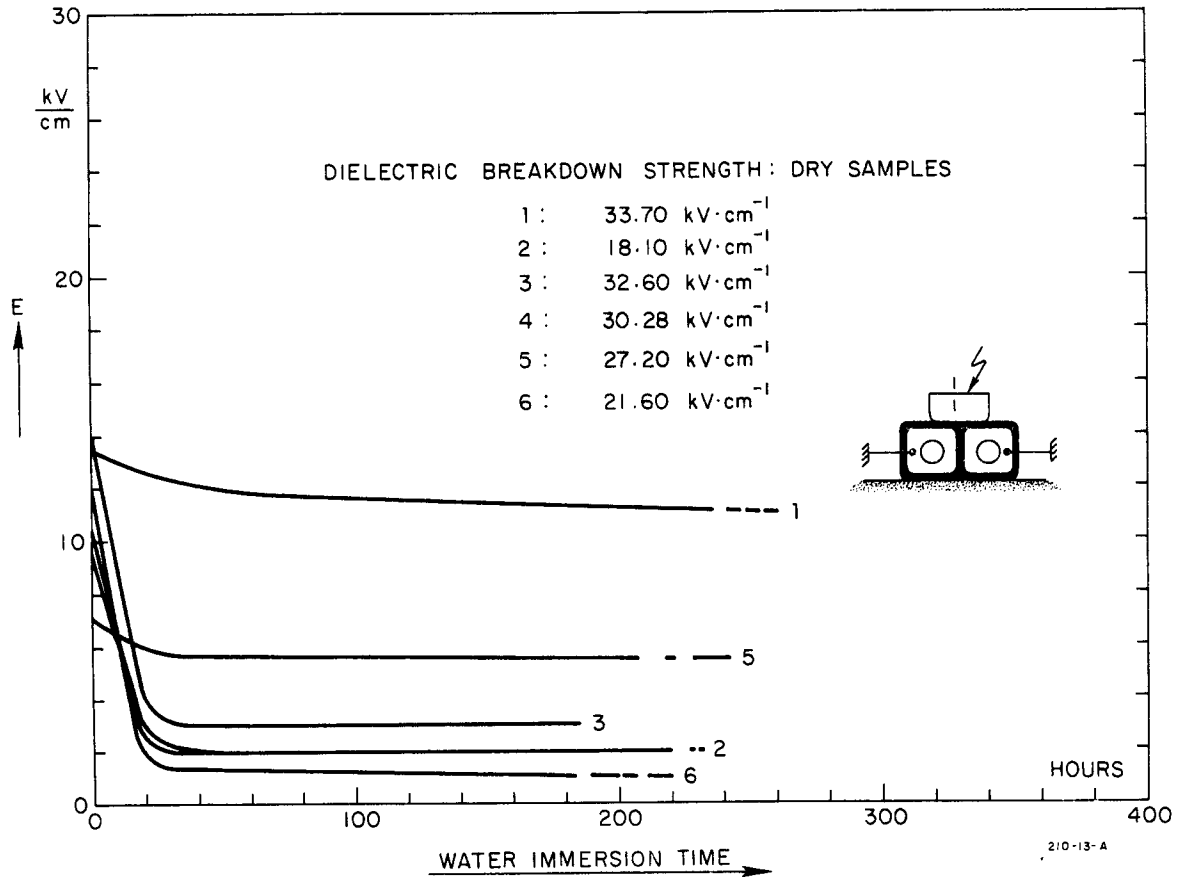

FIG. 18--Corona threshold of nonradiated and irradiated glass fiber reinforced, mineral-filled epoxies. (Samples immersed in 25°C tap water) (1) Nonradiated DER 332 LC and hardener DMA and MPDA; (2) irradiated absorbed dose 5×10^{12} ergs·gr^{-1}(binder as in 1); (3) irradiated absorbed dose 1.09×10^{14} ergs·gr^{-1} (binder as in 1); (4) irradiated absorbed dose 3.25×10^{14} ergs·gr^{-1} (binder as in 1); (5) nonradiated Epon 828/1031 and hardener NMA and BDMA; (6) irradiated absorbed dose 1.19×10^{14} ergs·gr^{-1} (binder as in 5).

The insulation resistance of glass fiber reinforced mineral filled epoxies samples (Fig. 16) as a function of absorbed irradiation dose was tested by simultaneous application of 500 volts dc between two insulated copper bars and electron irradiation. The leakage current was measured and recorded continuously as a function of absorbed irradiation dose shows that it follows the general rule of volume resistivity given in Fig. 15, curve 1 . The speculation that insulation materials become semi-conductors when exposed to irradiation energy could not be verified.

C. Moisture Absorption

The standard method of determination of water absorption by glass fiber laminates impregnated with resins was used: Samples not irradiated were dried at 110°C for 24 hours. Their weight and volume resistivity were determined. Afterwards they were immersed in tap water for 24 hours. The samples were dried with a dry cloth and their weight and volume resistivity were measured. These tests were repeated as a function of absorbed radiation dose. The increase in weight due to water absorption was recorded and compared with that of irradiated samples. The change in volume resistivity as a function of absorbed radiation dose of Al_2O_3-filled, glass fiber reinforced epoxies is given in Fig. 15. The increase in weight as a function of absorbed radiation dose is shown in Fig. 19. Comparing this to the test data given in Fig. 3, we observe an acceleration in moisture absorption, which leads to faster fatigue and electric breakdown of organic materials at lower electrical stress levels. An explanation of the greater affinity of irradiated glass fiber resin systems toward moisture absorption may be seen in the breaking of the organic binder around and along glass fibers. Capillary forces in cracks attract moisture and lead to faster fatigue.

D. Radiation Dosimetry

Among a variety of dosimetry methods, we chose the simple method of temperature rise in cooling water when passing through the irradiated sample to determine the total beam power absorbed by the irradiated sample. The amount of cooling water per second was measured accurately to 0.4% and was kept constant throughout the radiation tests. We measured (Fig. 20) the inlet and outlet water temperatures and recorded continuously the temperature fluctuations. The heat loss due to thermal radiation to the

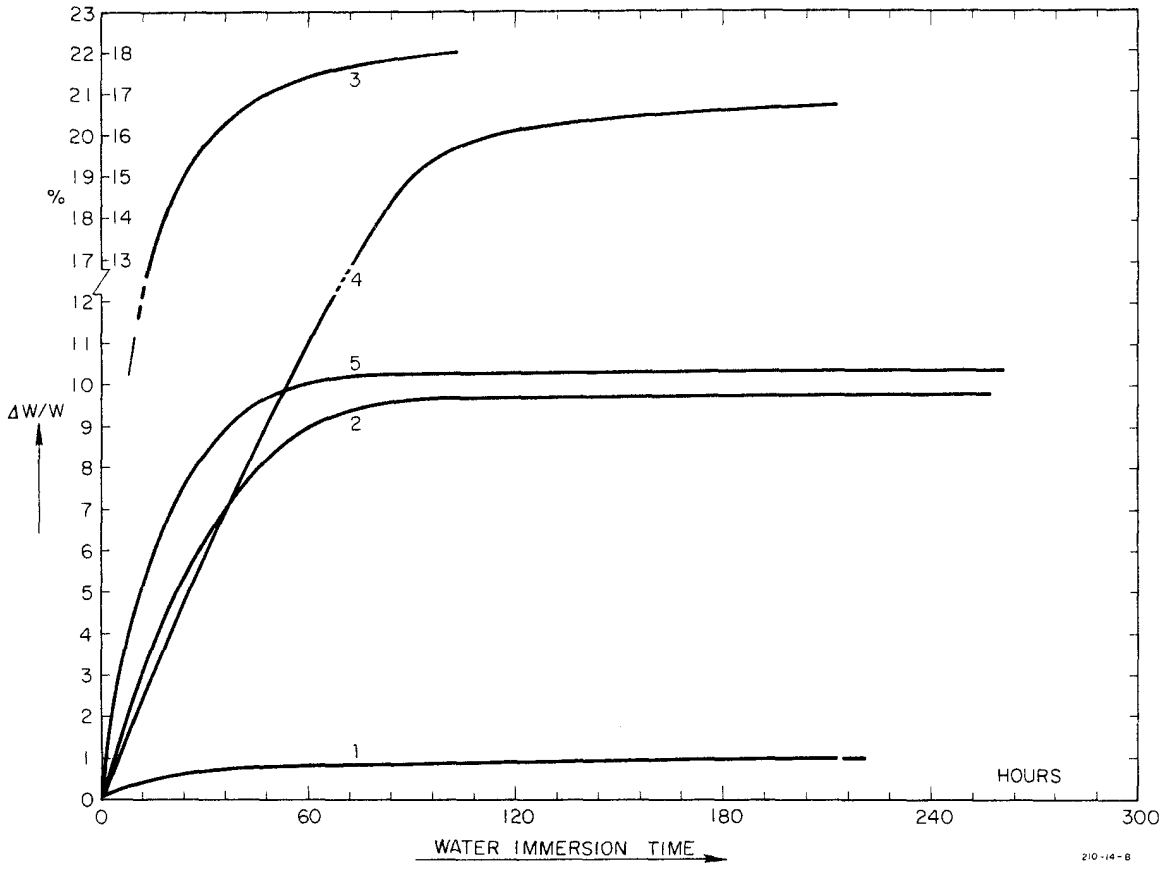

FIG. 19--Moisture absorption of glass fiber reinforced, mineral-filled epoxies of nonradiated and irradiated samples. (Sample immersed in 25°C tap water) (1) Nonradiated. DER 332 LC and hardener DMA and MPDA; (2) absorbed radiation 1.09×10^{14} ergs·gr^{-1} (binder as in 1); (3) absorbed radiation 3.25×10^{14} ergs·gr^{-1} (binder as in 1); (4) absorbed radiation 5×10^{12} ergs·gr^{-1} (binder as in 1). Tests carried on in an LRL pool-type reactor. Samples immersed in water during irradiation; (5) absorbed radiation 1.19×10^{14} ergs·gr^{-1} (binder 2850 FT and hardener 11).

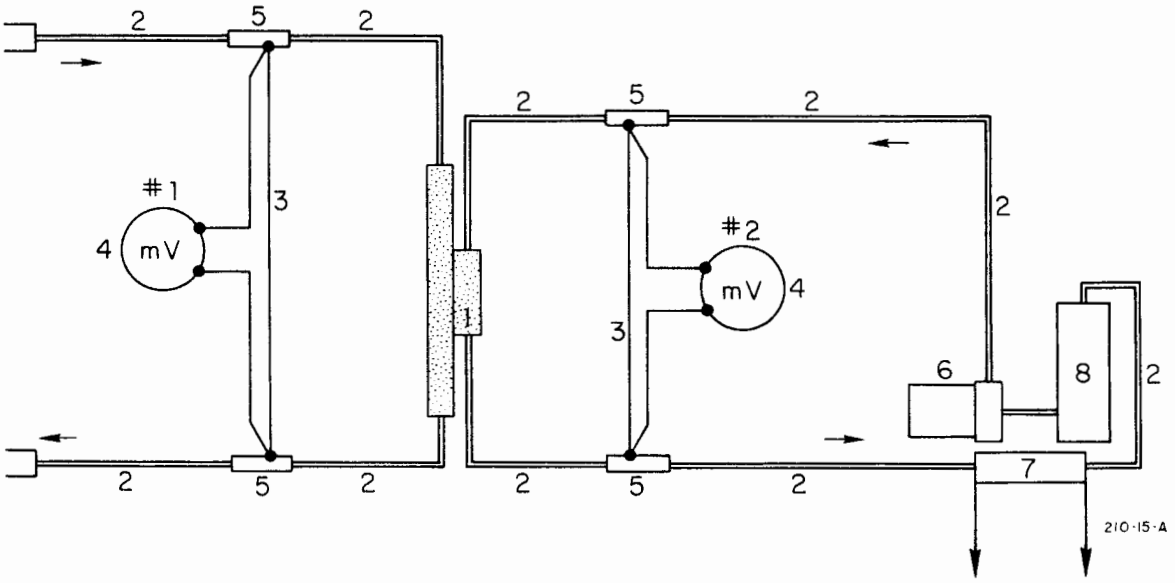

FIG. 20a--Schematic circuit diagram for testing absorbed radiation dose: (1) sample; (2) water tubing (polyethylene); (3) thermocouple; (4) millivolt meter; (5) copper tubing; (6) motor and pump; (7) heat exchanger; (8) water reservoir.

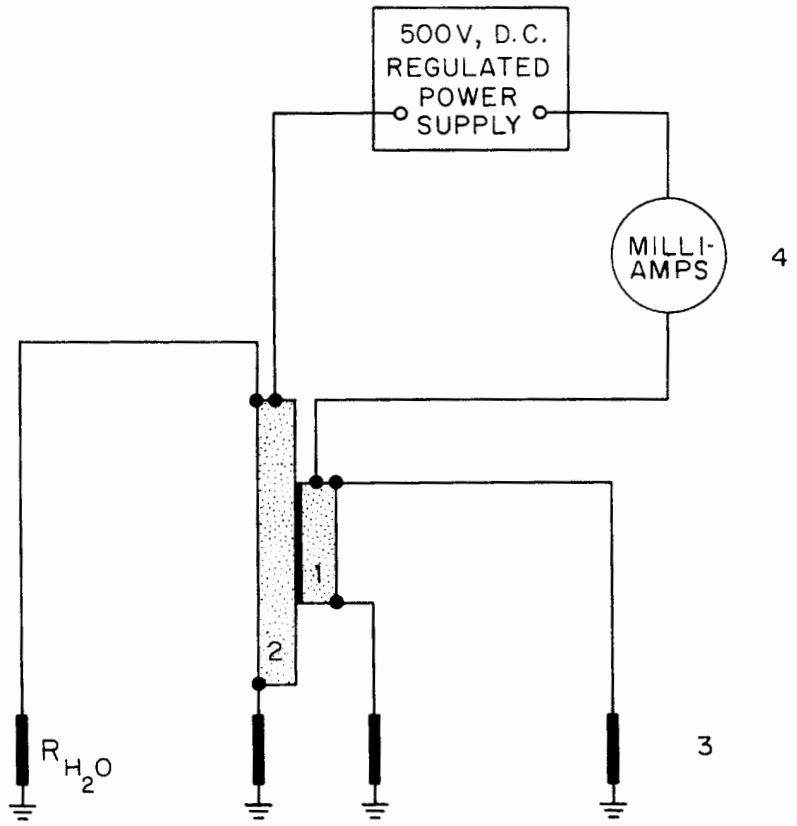

FIG. 20b--Schematic circuit diagram for testing absorbed radiation dose: (1) irradiated sample half; (2) irradiated sample half; (3) shunt to ground, water leakage path; (4) milliamp meter.

ambient can be neglected. The average incident beam current is measured with a current transformer and the beam flux passing through the sample was measured by means of a Faraday cup. Integration over the radiation period would result in measuring the incident beam power, the absorbed beam power by the sample, and the beam flux passing unabsorbed through the sample. The weight of the irradiated part of the sample was determined by planimetry of the discolored surface area of the sample and weight measurement of the sample. The accuracy of the radiation dose measurements is believed to be better than 5%.

E. Metallographic Techniques

The effect of electron beam irradiation on the insulation was investigated by metallographic techniques and x-ray diffraction methods. The experiments were intended to investigate whether reinforcing resins and filling them with inorganic materials can be interpreted as a result of irradiation-enhanced surface reaction of glass fiber, such as chemical reaction with alumina or devitrification.

Microscopic observation showed a peculiar optical interference around the highly irradiated glass fiber, which may have been due to structural change of the glass fiber and the filler (Figs. 21a and 21b). The x-ray diffraction method was utilized in order to investigate whether the surface reaction or devitrification has actually taken place.

In both tests the results are not conclusive. Owing to difficulties in obtaining a smoothly polished surface, no positive conclusions were possible. The x-ray diffraction method did not reveal any indication of a new phase formation.

However, as shown in Figs. 21a...21f, a bright fringe around the glass fiber is consistently observed only in the case of irradiated composites. This may be related to devitrification of the glass fiber, or a new crystallographic phase may have been formed by surface reaction. Because of technical difficulties in obtaining perfect surfaces, the interpretation is not conclusive. Crystallographic changes of the filler in the insulation composite are not conspicuous, but shrinkage due to decarburization of the epoxy resins is clearly noticed. The analysis of the x-ray diffraction pattern was made by composition of peak positions from each specimen. In a sense, all peaks were identified as those from α-alumina. The observed

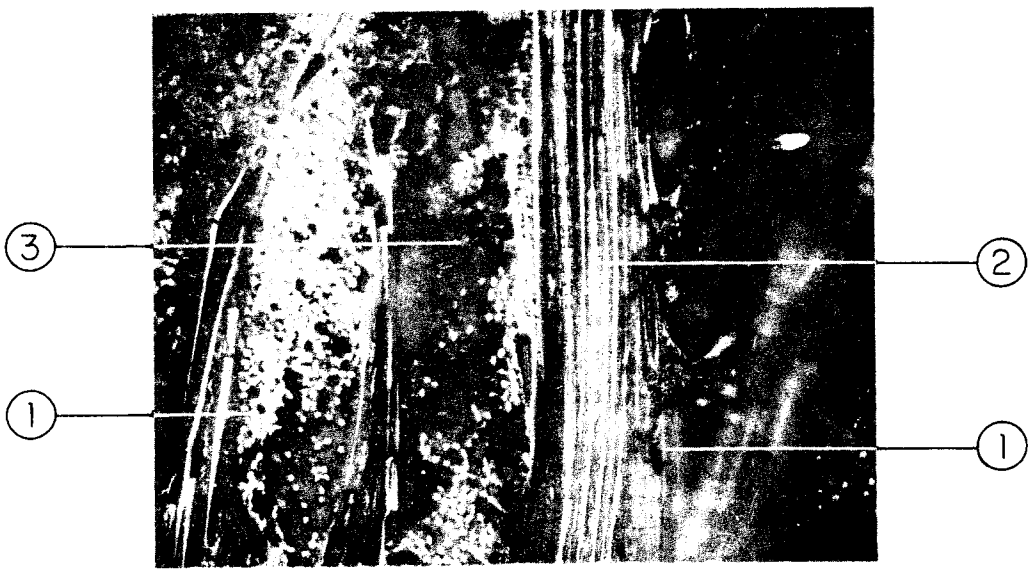

FIG. 21a--Irradiated glass fiber cloth impregnated with mineral-filled epoxy (magnification 140). Absorbed radiation dose 2×10^{13} ergs·gr^{-1}. (Fringe in glass fiber surface is visible) (1) Fiber filament; (2) fringe on fiber filament; (3) mineral-filled thermoset.

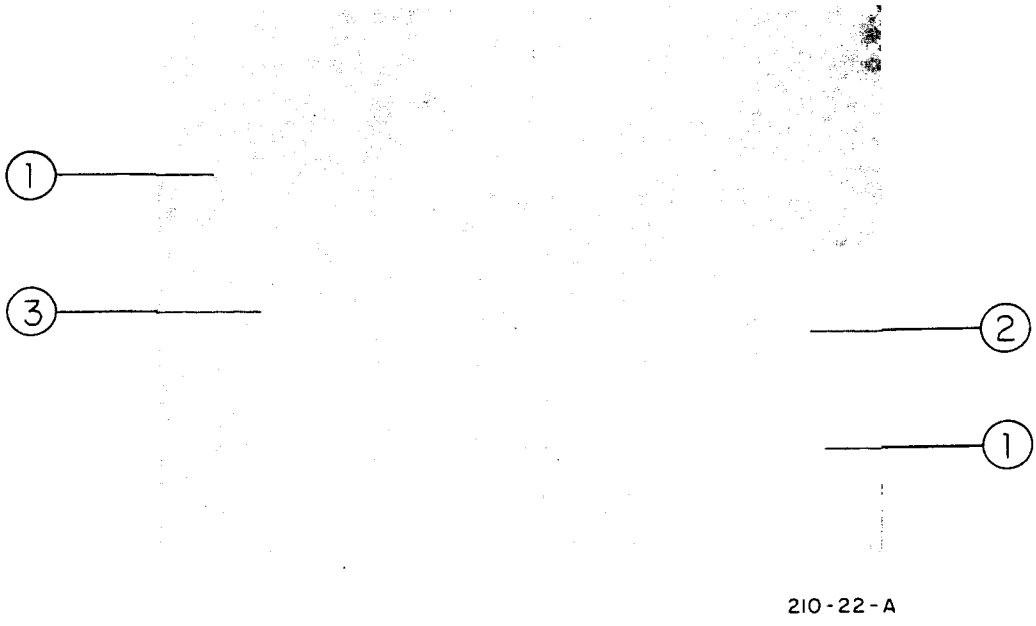

FIG. 21b--Irradiated sample (magnification 140). Absorbed radiation dose 5×10^{12} ergs·gr^{-1}. (1) Fiber filament; (2) fringe on fiber filament; (3) mineral-filled thermoset.

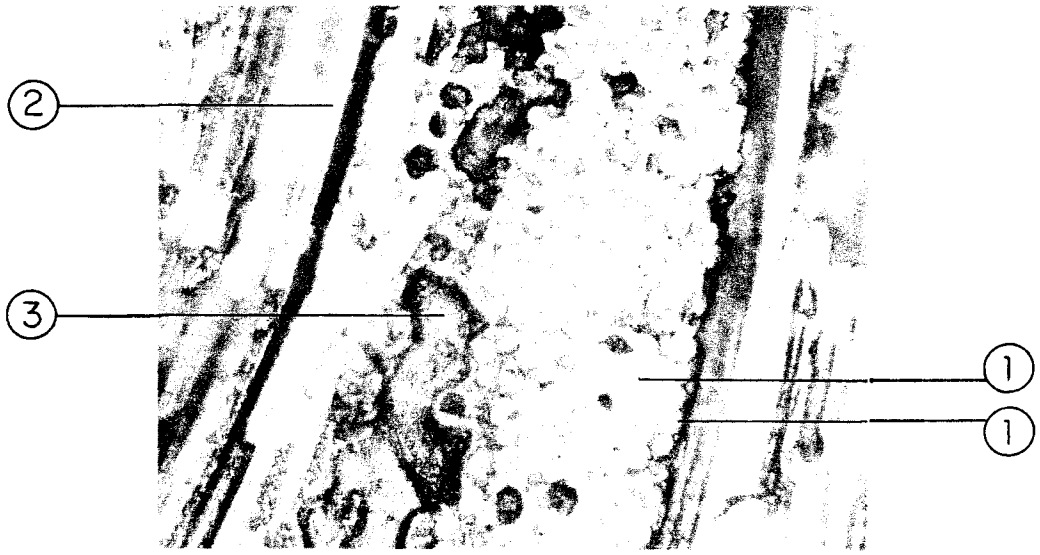

FIG. 21c--Irradiated sample (magnification 300). Absorbed radiation dose 2×10^{13} ergs·gr^{-1}. (Fringe in glass surface left) (1) Fiber filament; (2) fringe on fiber filament; (3) mineral-filled thermoset.

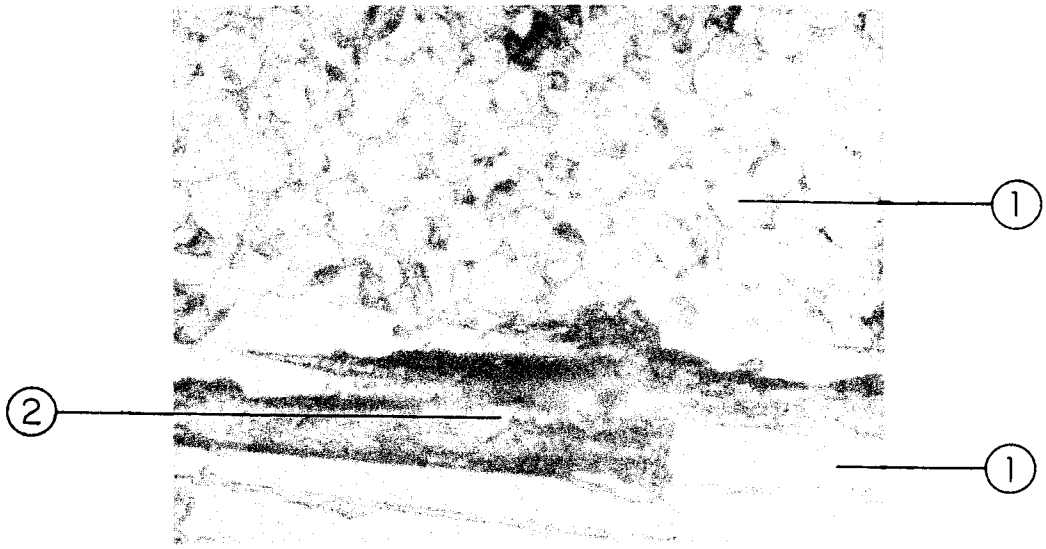

210-21-A

FIG. 21d--Non-irradiated sample (magnification 560). The partial wetting of the glass fiber surface with filled epoxy and the longitudinal fibers are visible. (1) Fiber filament; (2) mineral-filled thermoset.

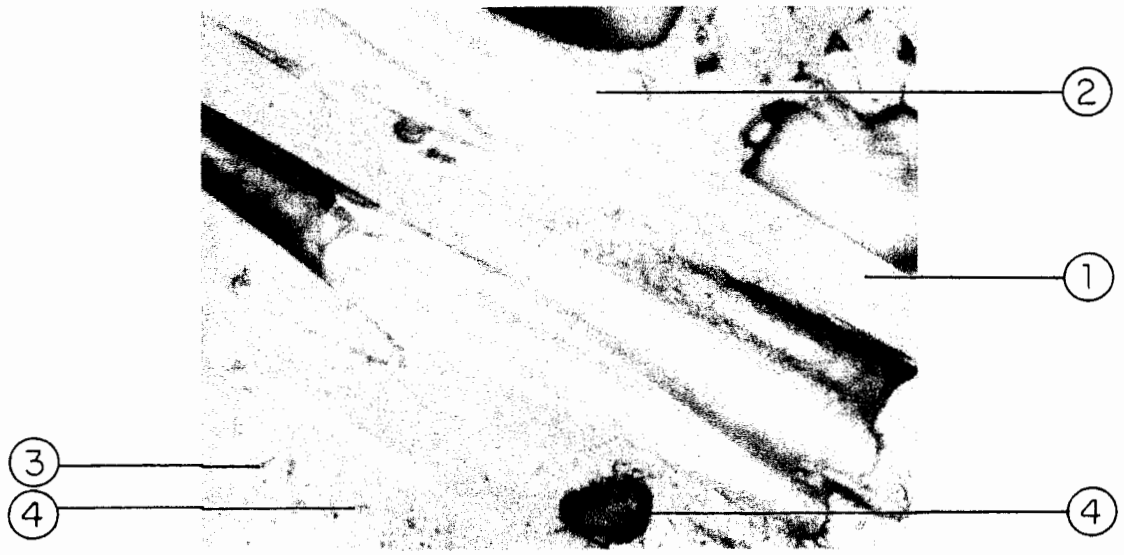

FIG. 21e--Irradiated sample (magnification 560). Irradiation dose 1.1×10^{14} ergs·gr^{-1} longitudinal cross section. (See fringe in glass surface) (1) Glass fiber; (2) fringe on fiber filament; (3) filler; (4) filled epoxy.

210-20-A

FIG. 21f--Non-irradiated sample (magnification 560). Epoxy and filler part. (1) Epoxy; (2) filler.

TABLE X

Diffraction peaks - α spacing in (Å)

Glass fiber[a]	Alumina filler[a]	α-Al_2O_3 ASTM 3-1033[b]	Intensity I/I_1	Miller index hk
3.503	3.476	3.43	80	10.2
2.561	2.547	2.55	80	10.4
2.475	2.378	2.35	70	11.1
2.092	2.088	2.06	100	20.0
1.744	1.739	1.73	80D	20.4,11.5
1.604	1.601	1.59	100	20.5
-	-	1.55	40	12.0
1.513	1.511	1.50	60	12.2
1.407	1.405	1.40	80	30.2
1.374	1.374	1.36	80	30.3
1.237	1.237	1.23	70	30.5
-	1.189	1.19	40	22.0
-	-	1.14	40D	22.2,31.0
-	-	1.12	40	31.2
-	-	1.09	50	22.5
-	1.080	1.07	60	31.4
1.043	1.042	1.04	70	31.5
-	-	1.01	20	40.1
0.9997	0.997	-	-	40.3

a) λ = 1.5405 Å (Cu K_α)

b) α-Al_2O_3 (alpha corundum) system: hexagonal a_o = 4.951, c_o = 12.97

data are listed in Table X and compared with data for α-Al_2O_3 listed in ASTM3-1033.

The transformation into a new crystalline phase would be detected effectively by a diffractometer. Since this was not the case, the possibility of a new phase formation by chemical reaction or devitrification

can be eliminated. This does not seem unreasonable if we consider the general effect of irradiation on chemical processes. The chemical effects of irradiation can be classified into two categories:[10]

a) effect on nucleation and diffusion;

b) effect on the chemical activity of solids in heterogeneous solid-gas and solid-liquid reactions.

It was experimentally derived that the diffusion coefficient under radiation (either electron or neutron) is of the order of $D = 10^{-20}$ cm^2/sec for α-brass.[11] For most metals, $D = 10^{-8} - 10^{-9}$ cm^2/sec at $T \approx 0.5\ T_m$. The bulk diffusion effect for $D = 10^{-20}$ cm^2/sec cannot be measured by conventional techniques. Enhanced effects in the case of solid-gas reactions are observed by different investigators, but knowledge is still fragmentary[12,13] and interpretations are non-existent. At any rate, solid-solid reactions which generally have higher activation energy could hardly be effected by the irradiation doses on our samples.

The interpretation of the higher radiation resistance due to reinforcement and filling must be sought in directions other than new phase formation and devitrification of glass or mineral filler.

A brief review of fracture theory is interesting in order to discuss the subject further.[14]

It has been derived that the theoretical tensile strength (i.e., fracture strength) σ_T is approximately 0.1 E, where E is Young's modulus. Actually the fracture strength is 10^{-2} to 10^{-3} of the theoretical value. The discrepancy was explained as an effect of flaws (microcracks) existing on the material surface. The fracture strength σ_F is given by the Griffith equation:

$$\sigma_F = (2E\gamma/\pi\ell)^{\frac{1}{2}} \quad , \tag{16}$$

where γ = specific surface energy and ℓ = half length of the crack. For inorganic glass,

$$E = 7.5 \times 10^5 \text{ kg} \cdot \text{cm}^{-2} \text{ (see Table II)} \tag{17}$$

and the theoretical tensile strength is

$$\sigma_T = 7.5 \times 10^4 \text{ kg cm}^2.$$

The actual tensile strength of glass is

$$\sigma_{Tac} = 2.9 \times 10^4 \text{ kg.cm}^2 \text{ (see Table II)} \qquad (18)$$

or less. The high value given in Table II is measured only for thin fibers. For larger glass fiber cross-sections,

$$\sigma_{Ta} = 7 \times 10^3 - 10^4 \text{ kg.cm}^2.$$

Because the depth of flaws on glass is comparable to the resolving power of a microscope (approximately 10 Å), the radiation-enhanced microdiffusion in localized areas may patch up the cracks.

At present, no data are available for radiation-enhanced microdiffusion in glass, but we may expect a diffusion coefficient of 10^{-20} cm^2/sec or higher because the mobility of atoms in glass is higher than in crystalline materials. It seems reasonable to say that the present reinforcement effect of glass fiber is correlated with "healing" of flaws during radiation. Based on this speculation, we may expect an even higher reinforcement effect by forming the glass fiber filler epoxy composit with more diffusible components, such as ground glass rather than alumina.

The filler grain size in the thermoset has a pronounced effect on radiation properties of the insulation system. Grain sizes of max. 10-20 microns were chosen as a compromise: The size of 0.5-1 microns improve radiation resistance further, but they are commercially difficult to obtain and extremely expensive in quantities to be used with coil insulations. In the range of 05-1 microns grain size the bond strength between filler and thermoset exceeds the covalent force between atom of the organic polymer and the structure is very stable with regard to radiation.

Another fact that must be considered is the intrinsic strength of the epoxy resin. The contribution to insulation strength from the resin is

apparently small after decarburization, but there must be some contribution from the intrinsic strength of resins at intermediate states. This can be easily seen from the retardation effects observed in our experiments.

F. Test Observations

At quite low irradiation doses, up to 10^{10} ergs·gr^{-1}, a discoloration of the sample surface is observed. Irradiated samples darken rapidly, which is probably due to initial stages of unsaturation effects. The color distribution over the beam spot is close to a Gaussian distribution. Increasing the dose turns the resin color to dark brown and gradually to black. The resin starts to degrade, filling the space between the inorganic filler and the glass fiber cloth with a black carbon powder (Fig. 21).

The inorganic filler, in our case pure alumina (Al_2O_3) crystals, appears as a white granular surface. Its appearance did not change in the case of DER 332 LC and Al_2O_3 filler up to the highest measured doses of 4.35×10^{14} ergs·gr^{-1}.

The alumina crystals are among the commonly used inorganic fillers and one of the most stable. At temperatures less than 100°C the irradiation of the alumina did not show any measurable dimensional changes. A bright fringe around the glass fibers is consistently observed only in irradiated samples. This may be related to devitrification of glass or to the formation of a new crystalline phase by surface reaction. Some dimensional changes in pure alumina filler are possible, but generally no mechanical changes were observable. Diffraction patterns did not disclose any signs of sintering of the alumina crystals. The filler stays in a rather loose form in the sample. It is known that the thermal and electrical conductivity of alumina decreases at high radiation doses ($> 10^{12}$ ergs·gr^{-1}). One interesting observation shows that the alumina is rather tightly bonded to the glass fiber even if there is no sign of any organic binder. This is assumed to be due to surface reactions and the intrinsic strength of the resins.

It is known that glass fiber reinforced and filled organic thermosettings are more radiation resistant than the unfilled thermosettings. The mechanical and electrical tests in the previous section show this very clearly. An explanation for the high radiation resistance cannot

be given with certainty at this time. However, the following explanations are possible:

a) Formation of more rigid structures.

b) Better distribution of the beam flux. A portion of the radiation energy is absorbed by the inorganic filler.

c) Devitrification of glass fiber, melting of the glass surface, and generation of a new bond between glass structure and inorganic filler.

d) Fillers with low sintering temperatures, such as glass powder, may sinter at temperatures below 100°C at high irradiation levels.

e) Evidence of sintering of the filler, although diffraction patterns and surface treatment did not verify this phenomena for some fillers.

f) Intrinsic strength of the resin.

It may be pointed out that after degradation of the organic thermosetting, no significant changes in the insulation structure were observed. The mechanical properties of the insulation are reduced by 90% of their original value and the remaining strength is primarily due to the glass fiber wrapped around the conductors. It seems feasible to increase the weight percentage of glass fiber in the insulation, in order to take advantage of the fiber strength and the devitrification and melting process in the glass structure.

V. MANUFACTURING PROBLEMS

The necessity of using highly filled thermosettings such as the above-described epoxies and low pressure silicones introduces a number of manufacturing problems, which may be described briefly in this chapter.

Filled thermosettings are quite viscous. The impregnation of medium weave glass fiber under vacuum introduces new problems, such as generation of voids, air pockets, and outfiltering of the filler by the glass fiber. Often the space between the conductors will not be filled with the loaded resin, specifically because of the filtering effect of the glass fiber cloth which permits wetting with resins but holds the filler back.

In order to achieve a uniform impregnation and casting, the following impregnation methods had to be applied.

1. Wet-Winding of the Pancakes

The conductor is cleaned and preheated to approximately 70°C. The alumina-filled epoxy is degassed (15 minutes under 400-600 microns vacuum). The epoxy is applied to the conductor surface by brushing or other means and simultaneously wrapped with medium or, better, tight weave glass fiber (type 181). It is recommended that 100-120 parts Al_2O_3 are used with 100 parts per weight of the epoxy. In this case it is required that the pot life of the applied epoxy be long, i.e., 24-36 hours. This means that only the curing agent BF_3MEA may be used, even if the radiation resistance of the impregnant is somewhat less than the aromatic agents. The coil should be heated to 60°C and vacuum should be applied to it in order to achieve a more uniform distribution of the epoxy. It is important that the resin does not cure. As ground insulation we recommend micafleece, glass fiber cloth which can be wet-wrapped around the coil using the alumina-loaded epoxy. The coil should be impregnated with pure DER332LC and the curring agent MPDA and MDA, pressed to the required size during the curing period. Prior to any impregnation the viscosity of the resin system must be checked at impregnation temperature. A uniform casting is possible only if the impregnation is performed with systems with viscosities below 1500 cP. The curing of the epoxies should be done in two steps: precuring 4-6 hours at 60°C; and postcuring 6 hours at 150°C. Magnet coils insulated for use in the beam switchyard area of the Stanford Linear Accelerator Center are shown in Figs. 22 and 23. The prototype of the beam switchyard 8 cm quadrupole utilizing the mineral filled epoxy for coil insulation in ceramic tubes in connection with braided stainless steel bellows for cooling passages are shown in Fig. 24.

2. Dry-Winding and Vacuum Impregnation

Coils are wound with dry, medium, or tight weave glass fiber tape and impregnated under vacuum with DER332LC, alumina filled (100 parts per weight of the epoxy system) using the curing agent MPDA and MDA.

The impregnation must occur in a closed mold with no side pressure applied to the coil. After impregnation, apply pressure to the coil sides and precure the coil. After a partial cure of the epoxy, apply the ground insulation (mica loaded, tight weave glass fiber tape) to the

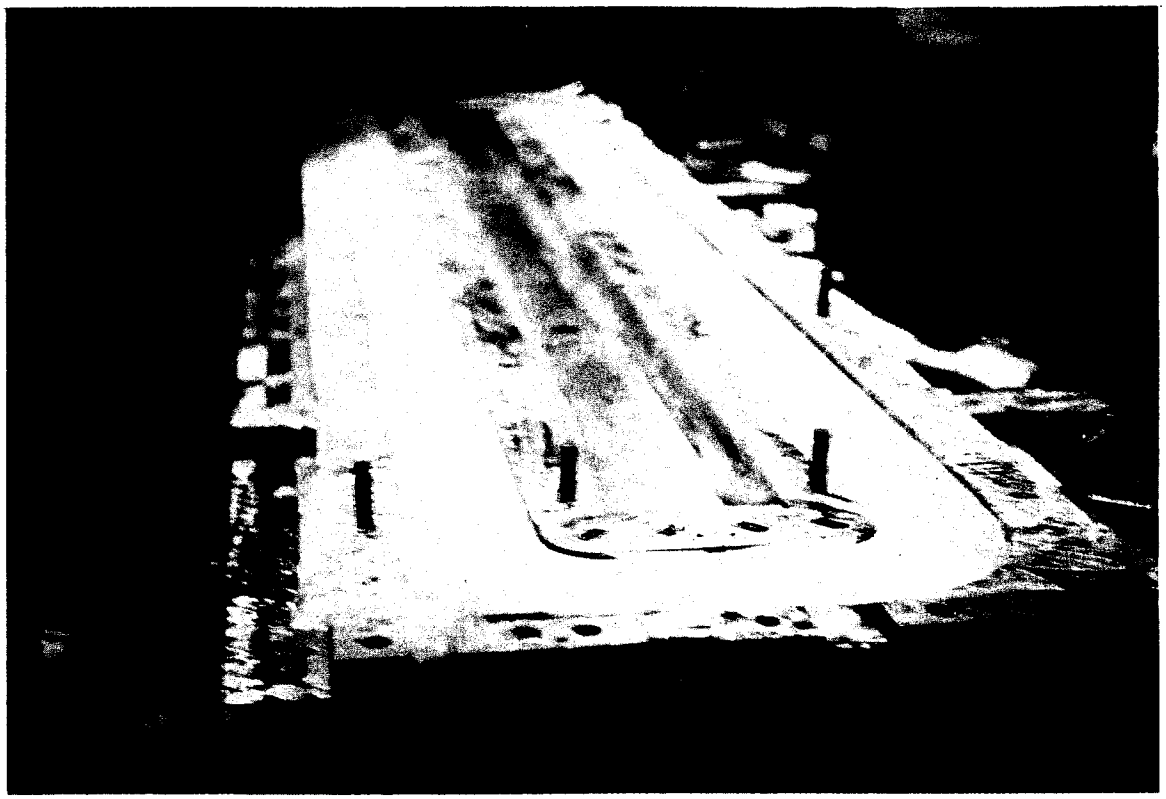

FIG. 22--Pancake of a bending magnet coil during winding and insulation. The conductor is wrapped in glass fiber tape and painted with filled epoxy during winding.

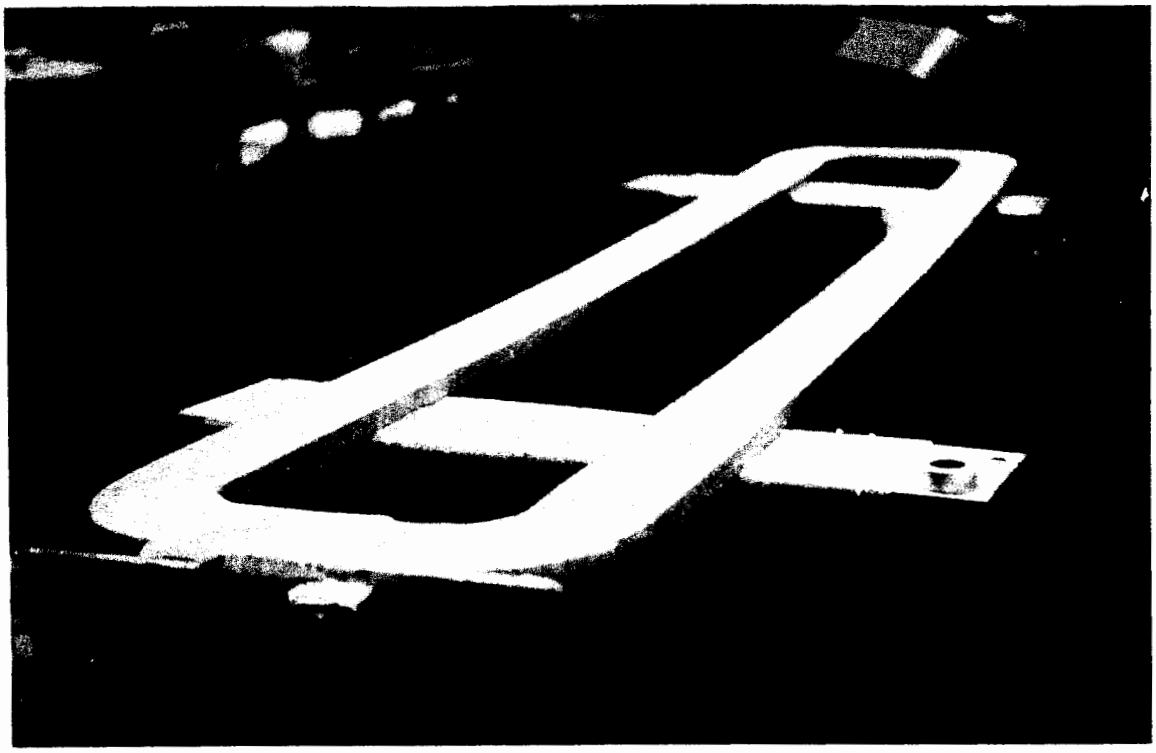

FIG. 23--Bending magnet double pancake with ground insulation. The double pancake is ready to be placed in the mold for final impregnation.

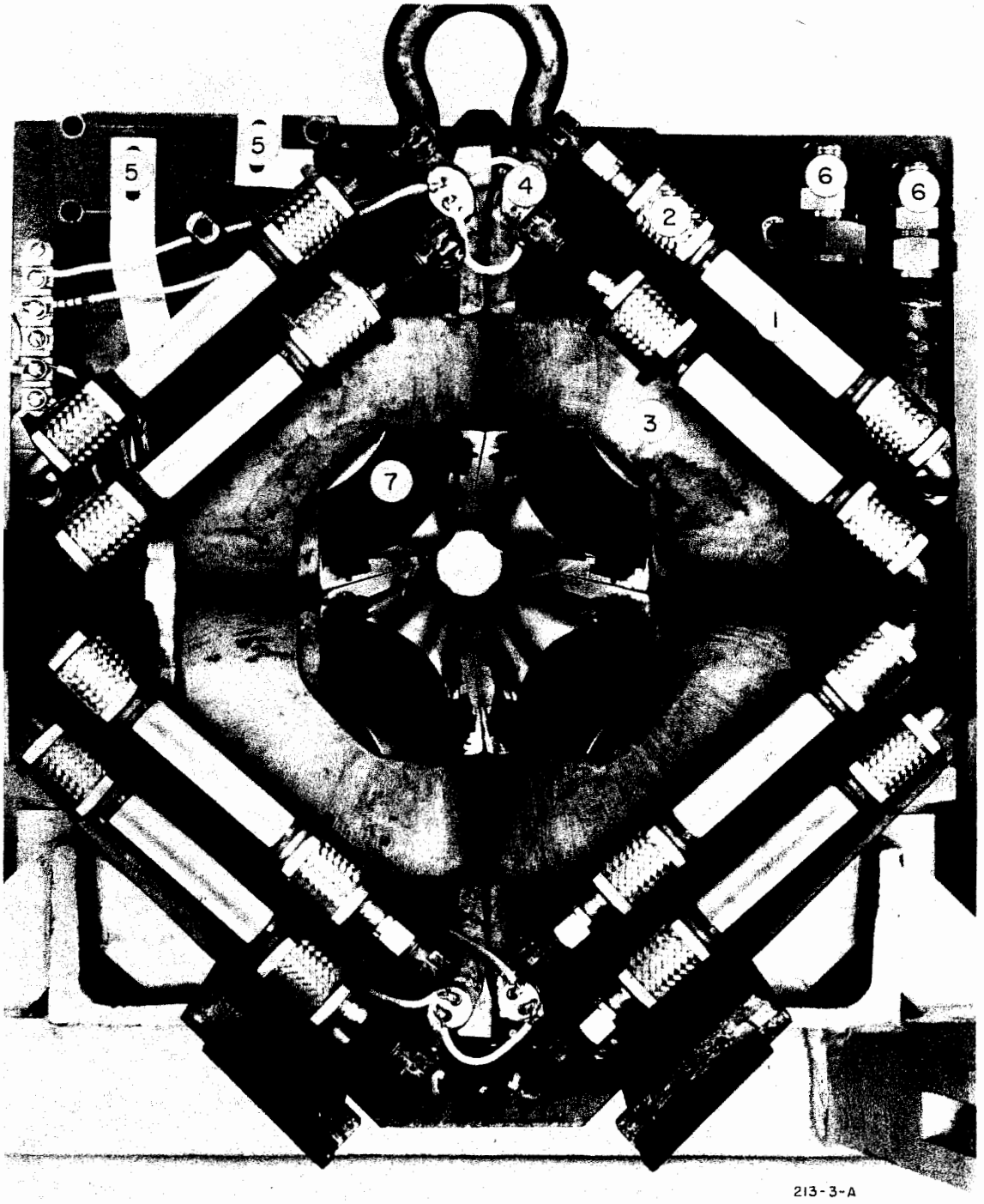

FIG. 24--8 cm quadrupole in the beam switchyard area. (1) Ceramic tubing; (2) bellows protected by brace; (3) coils; (4) thermoswitches; (5) electric bus bar; (6) water connection; (7) pole tips.

coil and impregnate under vacuum with DER 332 LC and curing agent MPDA and MDA. Cure the epoxy as follows: precuring 4-6 hours at 60°C; post-curing 6 hours at 150°C. It is essential that the coil surface be clean prior to the application of the ground insulation, in order to guarantee a good bond between coil body and ground insulation.

VI. CONCLUSIONS

Theoretical studies on absorbed radiation doses carried out for magnet coils located in the beam switchyard area of the Stanford University two-mile linear accelerator show that over a period of ten years the expected radiation dose may exceed, in the worst case, about 10^{13}-10^{14} ergs·gr^{-1}. Any exchange and replacement of magnets in the BSY area is difficult, expensive, and would mean a long delay in the experimental program. The coil insulation should be able to withstand at least the above radiation dose.

From a number of different promising epoxies used for magnet coil insulation tested at SLAC, we may conclude the following:

1. Glass fiber reinforced and mineral-filled epoxies show the highest radiation resistance compared to other organic resins.
2. Systems with the highest equivalent of epoxy per hardener and pure aromatic hardener give the best results. A certain excess of epoxy stabilizes the system to degradation.
3. Epoxy systems with high heat distortion temperatures are more stable.
4. Specific epoxy systems showing the best results were DER 332 LC with 18 parts per weight of MDA and MPDA hardener. This system reinforced with medium weave glass fiber cloth and filled with granular alumina retained 25-30% of its original mechanical properties at the absorbed radiation dose of 1.1×10^{14} ergs·gr^{-1}.
5. Blending of epoxies gives charred composites of 2-3 times the strength of the low viscosity epoxy used for impregnation, i.e., a mixture of DEN 438/DER 332 LC with the mix ratio of 1:3 and Epon 828/1031 with the mix ratio of 1:1 improves radiation resistance by a factor of approximately 2.

6. The addition of the wetting agent Dow Corning Z-6040 (1-2 parts per weight of epoxy) to the filler increases the mechanical strength even in excess of those for unfilled epoxies.
7. The glass fiber cloth (plain, medium, or tight weave) must be heat-cleaned and chemically treated (Volan A, Silane) to achieve optimum bond to the epoxy system. It is advisable that at least 25-30% of the insulation volume be occupied by glass fiber.
8. Fillers to be used for loading the organic resin are pure alumina, granulous, with a grain size of a maximum of 10 microns (equivalent to 900 mesh size), silica or ground glass.
9. Filler grain sizes of 0.5-1 microns improve radiation resistance compared to sizes mentioned under 8. However, due to price and availability a compromise seems to be reasonable.
10. Recommended insulation structures should contain:

Conductor Insulation

organic resin system	23-16	parts	per	weight
inorganic filler	27-19	"	"	"
glass fiber cloth	50-65	"	"	"

Ground or Main Insulation

organic resin	17-20	"	"	"
inorganic filler	13-15	"	"	"
micafleece	45	"	"	"
glass fiber cloth	25-20	"	"	"

If mica is not desired, the ground insulation will be the same as the conductor insulation.

11. To achieve void-free castings, the viscosity of the epoxy, curing agent, and filler system should not exceed 1000 cP at impregnation temperature.
12. Unfilled B-staged glass fiber epoxy systems are unsatisfactory. If B-staged systems are used, the glass fiber should be loaded with the resin and the filler.
13. Vacuum impregnation gives the best result if performed in closed molds where a uniform pressure may be applied to the coil insulation after the impregnation.

    If B-staged systems are used, it is recommended that the coil be evacuated after heat application.

14. Ceramic impregnants do not appreciably change their mechanical properties. However, their initial mechanical strength is low and unsatisfactory compared to epoxies. Ceramic systems have very low expansion coefficients, are brittle, and produce manufacturing difficulties. It is not recommended that they be used with large magnet coils.

15. Low viscosity silicone systems may be used for magnet coils if bond and compression are not essential. They show good radiation resistance.

16. DER 332 LC and hardner MPDA, MDA has a limited pot life of approximately 8-10 hours at 25°C. It is suitable for the impregnation of dry glass fibers under vacuum, but not suitable for wet-winding large coils due to the increase of viscosity to approximately 50,000 cP after being exposed to room temperature approximately 24 hours.

17. If a long pot life of several days and less radiation resistance is required, DER 332 and hardener BF_3MEA are suitable. They withstand radiation doses higher than 10^{13} ergs·gr^{-1} and show some gas evolution under high radiation bombardment. The mixture of the resin system with alumina filler and thixotropic material should not result in viscosity values higher than 2000 cP at 60°C.

18. The affinity for water absorption is increased by radiation. Water repellent coatings do help at low radiation levels. They are destroyed at maximum levels of 5×10^{12} ergs·gr^{-1}. Coils must be protected from water vapor and humidity.

Glass fiber reinforced and filled organic resins change their mechanical properties (bond strength, impact, and tensile strength) in the range of $10^{12} \leq r \leq 10^{15}$ ergs·gr^{-1}, as

$$\sigma_r = \frac{\sigma}{\sigma_o} = 1.944 + 1.7 \times 10^{-2} \log_{10} r - 1.074 \times 10^{-2} (\log_{10} r)^2 + 1.188 \times 10^{-3} (\log_{10} r)^3 - 8.026 \times 10^{-5} (\log_{10} r)^4 \quad (19)$$

And for mineral filled, not glass fiber reinforced epoxies in the radiation dose range of $8 \times 10^{10} < r < 10^{13}$ ergs·gr^{-1},

$$\sigma_r = \frac{\sigma}{\sigma_o} = 2.723 - 4.8 \times 10^{-3} (\log_{10} r) - 1.074 \times 10^{-2} (\log_{10} r)^2 - 3.07 \times 10^{-5} (\log_{10} r)^4 \qquad (20)$$

where r is the absorbed radiation dose in ergs·gr^{-1}. Below 10^{12} ergs·gr^{-1} no appreciable change in mechanical strength is observed. The dielectric strength is practically unchanged up to $r = 10^{13}$ ergs·gr^{-1}. At 3.25×10^{14} ergs·gr^{-1}, samples impregnated as shown above still retain 14% of their orignial bond strength.

ACKNOWLEDGEMENT

The author is indebted to Dr. J. Ballam, Dr. R. Taylor, Dr. H. DeStaebler and Dr. Z. Guiragossián, SLAC, and Dr. B. Hedin, CERN for their comments and many helpful suggestions. He is most grateful to Dr. P. Craven, Dow Chemical Company for reading the manuscript and for a number of corrections. To Mr. L. Johns, National Electric Coil for the performance of tests; to Dr. Kohn, General Electric Co. in Schenectady, New York, for the preparation of many samples; to R. Rummel, SLAC, who performed the radiation tests at Mark IV Stanford and to Prof. Dr. J. Shyne and Mr. T. Takahashi, Stanford Materials Science Dept. for the work of Section IV.E of this paper and to companies and manufacturers who helped during the tests with suggestions and sending samples of their products.

LIST OF REFERENCES

1. W. J. Eakins, The Interface: The Critical Region of a Composite Material (to be published).
2. S. O'Leesky and G. Mohr, Handbook of Reinforced Plastic (Reinhold Publishing Co., New York, 1964.)
3. A.M. Paquin, Epoxyd verbindungen und epoxydharze (Springer-Verlag, Berlin, 1958).
4. B. Rossi, High-Energy Particles (Prentice-Hall, New York, 1953).
5. I. E. Tamm and S. Belenky, J. Phys. USSR 1, 177 (1939).
6. Z. Guiràgossiàn, "Longitudinal and radial distribution of shower development in Cu, H_2O and Al," Internal Report, Stanford Linear Accelerator Center, Stanford University, Stanford, California (1963).
7. J. F. Kircher and R. E. Bowman, Effects of Radiation on Materials and Compounds (Reinhold Publishing Co., New York, 1964).
8. R. W. King, N. J. Broadway and S. Palinckak, "The effect of nuclear radiation on elastomeric and plastic components and materials," REIC Report No. 21, Radiation Effects Information Center, Battelle Memorial Institute, Columbus, Ohio (1961).
9. C. D. Bopp and O. Sisman, "Radiation stability of plastics and elastomers," ORNL Report No. 1373, Oak Ridge National Laboratory, Oak Ridge, Tennessee (1953).
10. G. J. Dienes, in Proc. 4th International Symposium on Reactivity of Solids (ed. J. H. DeBoer), American Elsevier, New York (1961); p. 417.
11. A. C. Damask, in Proc. 4th International Symposium on Reactivity of Solids (ed. J. H. DeBoer), American Elsevier, New York (1961); p. 479.
12. W. H. Cropper, Science 137, 955 (1962).
13. W. L. Kosiba and G. J. Dienes, in Advances in Catalysis and Related Subjects, Vol. 9 (Academic Press, New York, 1957); p. 398.
14. J. P. Berry, in Modern Aspect of the Vitreous State (ed. J. D. MacKenzie), Vol. 2 (Betterworths, London, 1962); p. 114.

LEGAL NOTICE